ผลของการเผาผนึกด้วยไมโครเวฟและการเติมเซอร์โคเนียต่อโครงสร้างจุลภาคและการส่งผ่านแสงของอะลูมินาเซรามิก

นางสาว จุตินันท์ ไกรเกรอะ

วิทยานิพนธ์นี้เป็นส่วนหนึ่งของการศึกษาตามหลักสูตรปริญญาวิทยาศาสตรมหาบัณฑิต
สาขาวิชาเทคโนโลยีเซรามิก ภาควิชาวัสดุศาสตร์
คณะวิทยาศาสตร์ จุฬาลงกรณ์มหาวิทยาลัย
ปีการศึกษา 2549
ISBN 974-14-2052-8

EFFECTS OF MICROWAVE SINTERING AND ZrO_2 ADDITION ON MICROSTRUCTURE AND OPTICAL TRANSMITTANCE OF Al_2O_3 CERAMIC

Miss Jutinun Kraikrer

A Thesis Submitted in Partial Fulfillment of the Requirements

for the Degree of Master of Science Program in Ceramic Technology

Department of Materials Science

Faculty of Science

Chulalongkorn University

Academic Year 2006

ISBN 974-14-2052-8

Thesis Title	EFFECTS OF MICROWAVE SINTERING AND ZrO_2 ADDITION ON MICROSTRUCTURE AND OPTICAL TRANSMITTANCE OF Al_2O_3 CERAMIC
By	Miss Jutinun Kraikrer
Field of Study	Ceramic Technology
Thesis Advisor	Professor Shigetaka Wada, Ph.D.
Thesis Co-advisor	Assistant Professor Sirithan Jiemsirilers, Ph.D.

Accepted by the Faculty of Science, Chulalongkorn University in Partial Fulfillment of the Requirements for the Master 's Degree

.....Dean of the Faculty of Science

(Professor Piamsak Menasveta, Ph.D.)

THESIS COMMITTEE

.....Chairman

(Associate Professor Saowaroj Chuayjuljit)

.....Thesis Advisor

(Professor Shigetaka Wada, Ph.D.)

.....Thesis Co-advisor

(Assistant Professor Sirithan Jiemsirilers, Ph.D.)

.....Member

(Associate Professor Supatra Jinawath, Ph.D.)

.....Member

(Dujreutai Pongkao Kashima, D.Eng.)

จุตินันท์ ไกรเกรอะ : ผลของการเผาผนึกด้วยไมโครเวฟและการเติมเซอร์โคเนียต่อโครงสร้างจุลภาคและการส่งผ่านแสงของอะลูมินาเซรามิก. (EFFECTS OF MICROWAVE SINTERING AND ZrO_2 ADDITION ON MICROSTRUCTURE AND OPTICAL TRANSMITTANCE OF Al_2O_3 CERAMICS) อ. ที่ปรึกษา : ศาสตราภิชาน ดร. ชิเกทากะ วาดะ, อ.ที่ปรึกษาร่วม : ผศ. ดร. ศิริธันว์ เจียมศิริเลิศ 72 หน้า. ISBN 974-14-2052-8

งานวิจัยนี้ศึกษาผลของการเผาผนึกด้วยไมโครเวฟเปรียบเทียบกับการเผาผนึกแบบดั้งเดิมและผลของการเติมสารเติมแต่งเซอร์โคเนียต่อโครงสร้างจุลภาคและสมบัติของอะลูมินาโปร่งใส โดยมุ่งเน้นให้ชิ้นงานอะลูมินาเซรามิกมีความโปร่งใสมากยิ่งขึ้นด้วยการลดขนาดของเกรนให้อยู่ในระดับซับไมครอน ในงานวิจัยใช้ผงอะลูมินาเป็นสารตั้งต้น ขึ้นรูปชิ้นงานโดยการอัดสองทิศทางด้วยแรงอัด 20 เมกะพาสคาล และต่อจากนั้นนำไปให้ความดันทุกทิศทางแบบเย็น ด้วยแรงอัด 200 เมกะพาสคาล เผาผนึกด้วยอุณหภูมิ 1300-1500 องศาเซลเซียส เป็นเวลา 2 ชั่วโมง หลังจากนั้นทำการเผาผนึกโดยการให้ความดันทุกทิศทางแบบร้อนด้วยอุณหภูมิ 1250-1300 องศาเซลเซียส เป็นเวลา 0.5 1 และ 2 ชั่วโมง ภายใต้ความดันแก๊สอาร์กอน 150 เมกะพาสคัล

การเผาผนึกด้วยไมโครเวฟจะใช้เวลาสั้นกว่าการเผาผนึกด้วยวิธีดั้งเดิม และเร่งให้เกิดความหนาแน่นเร็วขึ้นแต่ไม่ได้มีความหนาแน่นสูงกว่าการเผาผนึกแบบดั้งเดิม ชิ้นงานที่ได้จากการเผาผนึกด้วยไมโครเวฟมีการส่งผ่านของแสงต่ำกว่าชิ้นงานที่ได้จากการเผาผนึกแบบดั้งเดิมซึ่งมีสาเหตุมาจากขนาดของเกรนมีการกระจายตัวไม่สม่ำเสมอค่อนข้างสูง ภาวะที่เหมาะสมสำหรับการเผาผนึกโดยการให้ความดันทุกทิศทางแบบร้อน คือที่อุณหภูมิ 1300 องศาเซลเซียส เป็นเวลา 0.5 ชั่วโมง ด้วยอัตราการให้ความร้อน 10 องศาเซลเซียสต่อนาที ผสมผงเซอร์โคเนียในปริมาณ 0 0.2 และ 0.4 เปอร์เซ็นต์โดยน้ำหนักลงในผงอะลูมินาซึ่งมีผงแมกนีเซียผสมอยู่ด้วย 0.03 เปอร์เซ็นต์โดยน้ำหนัก การเติมเซอร์โคเนียสามารถยับยั้งการโตของเกรนอะลูมินาเซรามิกแต่ส่งผลกระทบต่อความหนาแน่น ในการเผาผนึกชิ้นงานที่เติมแต่งด้วยเซอร์โคเนียให้มีความหนาแน่นเท่ากับชิ้นงานที่ไม่ได้เติมนั้นจะต้องใช้อุณหภูมิที่สูงขึ้น ขนาดเกรนของชิ้นงานที่มีความหนาแน่นสูงที่เติมแต่งด้วยเซอร์โคเนียนั้นเล็กกว่าชิ้นงานที่ไม่ได้เติมเซอร์โคเนียเพียงเล็กน้อยเท่านั้น ดังนั้นชิ้นงานที่เติมแต่งด้วยเซอร์โคเนียจึงไม่แสดงสมบัติการส่งผ่านของแสงได้ดีกว่าชิ้นงานที่ไม่ได้เติม

ภาควิชา วัสดุศาสตร์	ลายมือชื่อนิสิต จุตินันท์ ไกรเกรอะ
สาขาวิชา เทคโนโลยีเซรามิก	ลายมือชื่ออาจารย์ที่ปรึกษา S. Wada
ปีการศึกษา 2549	ลายมือชื่ออาจารย์ที่ปรึกษาร่วม Shirut J.

4772252423 : MAJOR CERAMIC TECHNOLOGY

KEY WORD: TRANSPARENT ALUMINA / ZIRCONIA ADDITION / MICROWAVE SINTERING

JUTINUN KRAIKRER : EFFECTS OF MICROWAVE SINTERING AND ZrO_2 ADDITION ON MICROSTRUCTURE AND OPTICAL TRANSMITTANCE OF Al_2O_3 CERAMIC. THESIS ADVISOR : PROF. SHIGETAKA WADA, Ph.D., THESIS COADVISOR : ASST. PROF. SIRITHAN JIEMSIRILERS, Ph.D., 72 pp. ISBN 974-14-2052-8.

The objectives of this research are to study the effect of microwave sintering comparing with conventional sintering and the effect of zirconia addition on microstructure and optical transmittance of transparent Al_2O_3 ceramic. The experiment was concentrated on increasing the transmittance of Al_2O_3 ceramic by reducing grain size of Al_2O_3 to submicron level. Al_2O_3 powder was used as raw material. Green samples were prepared by biaxial hydraulic pressing with 20 MPa and followed by Cold Isostatic Press (CIP) of 200 MPa. Sintering was performed at temperatures ranging from 1300 to 1500°C for 2 hr followed by Hot Isostatic Press (HIP) at temperatures ranging from 1250 to 1300°C for 0.5, 1 and 2 hr with pressure of 150 MPa under Ar atmosphere.

Microwave sintering resulted in the fast processing time and accelerated densification to sinter Al_2O_3 ceramic, but did not show the higher density than that of conventional sintering. The transmittance of microwave sintered specimens was lower than that of conventional one because of the larger grain size distribution. The optimum HIP condition selected from the results was 1300°C for 0.5 hr with a heating rate of 10°C/min.

Zero, 0.2, and 0.4 wt% of ZrO_2 were added to Al_2O_3 powder together with 0.03 wt% of MgO. ZrO_2 addition inhibited grain growth of Al_2O_3 grain. However, it also disturbed densification. The sintering temperature of Al_2O_3 with ZrO_2 to attain the same high density shifted to higher temperature than Al_2O_3 with no ZrO_2 composition. Then the grain size of the full density specimen with ZrO_2 was a little larger than that without ZrO_2. As a result, better optical transmittance was not attained from the composition with ZrO_2.

Department :	Materials Science	Student's Signature	จุติน์นันท์ ไกรเกร:
Field of Study :	Ceramic Technology	Advisor's Signature	S. Wada
Academic Year :	2006	Co-advisor's Signature	Sirithan J.

ACKNOWLEDGEMENTS

I would like to express my gratitude to my advisor, Professor Dr. Shigetaka Wada, for his encouragement and valuable suggestions. His advises are very helpful and also inspired me to do this research. I would like to extend my gratitude to my thesis co-advisor, Asst. Prof. Dr. Sirithan Jiemsirilers, who helped me to solve scholarship problem and also life problem, for her useful guidance and suggestions. I really appreciate all the help that she gave me.

I would like to acknowledge Assoc. Prof. Tawatchai Charinpanikul, Asst. Dr. Varong Pavarajarn, and Mr. Nirut Wangmuklang for their helpful suggestions.

Furthermore, I would like to thank the National Nanotechnology Center (NANOTEC), National Science and Technology Development Agency (NSTDA), and Research Unit of Advanced Ceramics Chulalongkorn University for financial support.

I would like to thank TAKASAGO INDUSTRY CO., LTD, Thailand Institute of Science and Technology Research (TISTR), and Scientific and Technological of Research Equipment Center (STREC) for equipment support.

In addition, I am thankful to all my friends at the Department of Materials Science especially Mink and P'Tum for their friendship and warm collaborations. I am also thankful to P'Chok, who gave me willpower and love.

Finally, I would like to express my gratitude to my family especially my parents. The biggest inspirations for me have been my parents. They have always been extremely supportive and encouraging.

CONTENTS

Page

LIST OF TABLES

Page

LIST OF FIGURES

Page

CHAPTER I

INTRODUCTION

1.1 Background

In general, Al_2O_3 ceramic have been used in many industries such as insulator, structural materials, and high pressure sodium lamp. The production of dense ceramic parts with submicrometer grains and flawless microstructure is still one of the most challenging objectives in modern ceramic technologies [1]. Usually, Al_2O_3 ceramic are opaque and not a transparent material. Transparent Al_2O_3 ceramic can be produced either in single crystal or polycrystalline forms. Polycrystalline transparent Al_2O_3 ceramic is easier to produce than single crystal [2].

Sintering is the key process to obtain high transparent material. Microwave sintering is a promising technique for the densification of fine-grained ceramics which is fundamentally different from the conventional sintering. The advantage of microwave sintering compares to conventional heating is that heat is generated in the bulk of specimen. As a result, higher heating rate is possible without excessive temperature gradients. Higher heating rates are usually favored for densification without grain coarsening. As a result high density can be achieved with fine grain structure. Furthermore, microwave sintering has the potential to save firing energy.

In recent years, the remarkable technology progresses of transparent Al_2O_3 ceramic have been developed. To make polycrystalline transparent Al_2O_3 ceramic, submicron or nanometer size of Al_2O_3 powder and MgO additives are used [3]. In order to obtain a high transmittance and mechanical strength, the grain size of Al_2O_3 ceramic needs to be reduced to submicron level. Therefore, we are interested in the effect of ZrO_2 addition. In general, ZrO_2 is used as a refractory material, oxygen sensors, fuel cells and ceramic coatings [4]. ZrO_2 is already known to be used as the grain growth inhibitor for transparent Al_2O_3 ceramic. However, the effect is not reported widely.

The purpose of this research is to increase transmittance of Al_2O_3 ceramic by reducing Al_2O_3 grain size to submicron level. In the present study, high purity Al_2O_3 powder is used as raw material, MgO and ZrO_2 powders are used as additives. The effect of ZrO_2 addition for suppressing the grain growth of sintered Al_2O_3 ceramic will be discussed.

Fine alumina powder is sintered by microwave heating and conventional heating. The comparison of microwave and conventional sintering in microstructure, densification, grain growth, and transparency of Al_2O_3 ceramic are investigated. The sintering parameters, such as sintering temperature, soaking time, and heating rate are also discussed.

.

1.2 The objectives of research

1. To study the effect of microwave sintering comparing with conventional sintering on the microstructure and optical transmittance of Al_2O_3 ceramic.
2. To study the effect of zirconia addition as the grain growth inhibitor of transparent Al_2O_3 ceramic.

CHAPTER II

LITERATURE REVIEWS

2.1 Transparent polycrystalline Al_2O_3 ceramic

Al_2O_3 has been widely used as the structural material, for example IC substrates, refractory materials, and high pressure sodium lamp housing, due to its good properties, such as good corrosion and heat resistance, excellent chemical stability, low electrical conductivity, and high mechanical strength [5]. In addition, Al_2O_3 has been used as armor part. One approach to reduce the weight of part is the use of ceramics such as Al_2O_3, SiC and B_4C, which offer exceptional protection for very light weight [6]. Transparent Al_2O_3 ceramic can be prepared either in single crystal (sapphire) or polycrystalline form. The cost to manufacture polycrystalline transparent Al_2O_3 is lower than that of single crystal and easier to produce in production scale. Polycrystalline translucent Al_2O_3 has been available for optical applications since the early 1960s when Coble [7] invented translucent alumina, which has become a key element in high-pressure sodium vapor lamp and other optical instruments manufactured all over the world.

At present many researchers know that the polycrystalline transparent Al_2O_3 is made via powder processing using high purity and fine particle Al_2O_3 powder with addition of small amount of MgO as grain growth inhibitor and it can be sintered to pore-free state. In order to increase the transmittance of Al_2O_3, its optical anisotropy, the scattering at the grain boundaries and pores, the amount of light absorption at the second phase and impurities, and the reflection at the surface should be reduced [5,8]. The light-scattering mechanism is schematically illustrated in Fig. 2.1 [9]. Therefore, polycrystalline transparent Al_2O_3 ceramic must be produced to get the highest density with minimum porosity, followed by well polishing of the surface.

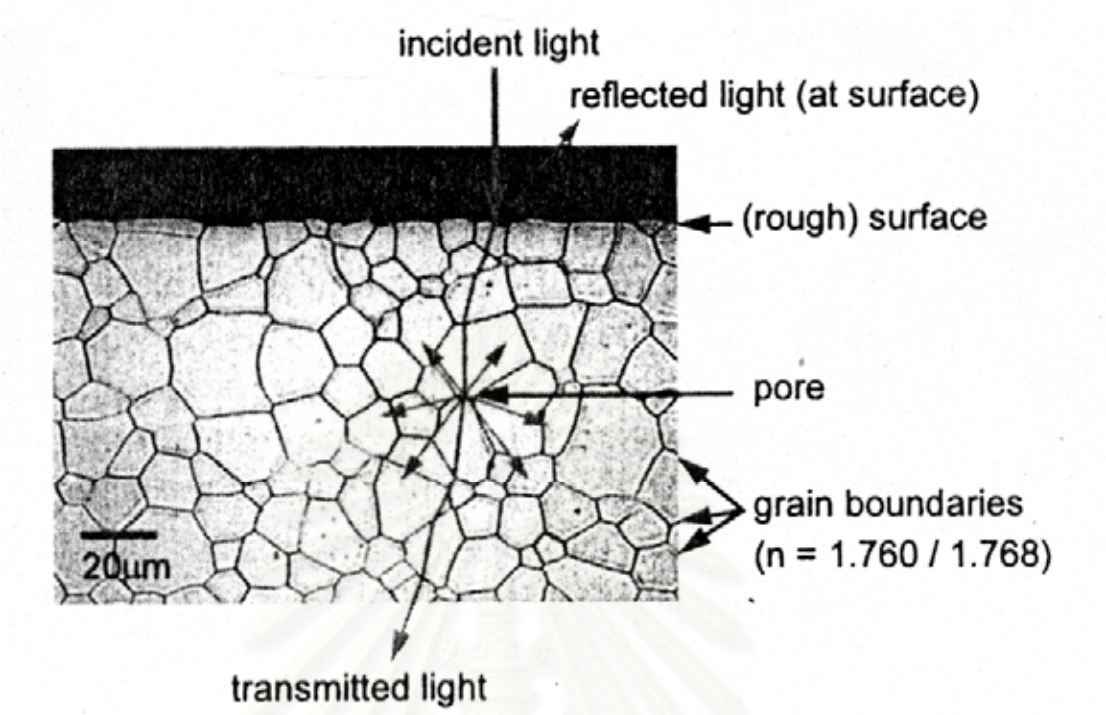

Fig. 2.1 Light-scattering mechanisms in the translucent polycrystalline Al_2O_3 [9]

2.2 Microwave sintering

Sintering is the most important step in the fabrication process of ceramics. During sintering, densification, recrystallization, and grain growth occur at the same temperature range. Microwave sintering is one of the new technologies to sinter ceramics. The technology has been reported in several proceedings starting from 1988. By controlling the properties of starting material, transparent ceramics have been produced, and this has been extended later to alumina and other ceramics [10]

2.2.1. Interaction of microwave with matter

Sutton [11] reported that the electrical and magnetic properties of a material determine whether microwave radiation can be transmitted, absorbed, or reflected as shown in Fig. 2.2. Most of the electrically insulating (dielectric) ceramics such as Al_2O_3, MgO, SiO_2, and glasses are transparent to microwave at room temperature, but when heated to a critical temperature T_c, they become good microwave absorbers. Other ceramics such as Fe_2O_3, Cr_2O_3, and SiC absorb microwave radiation more efficiently at room temperature. The addition of microwave-absorbing second phase to ceramics that are microwave transparent can greatly enhance the interaction of the system with microwave.

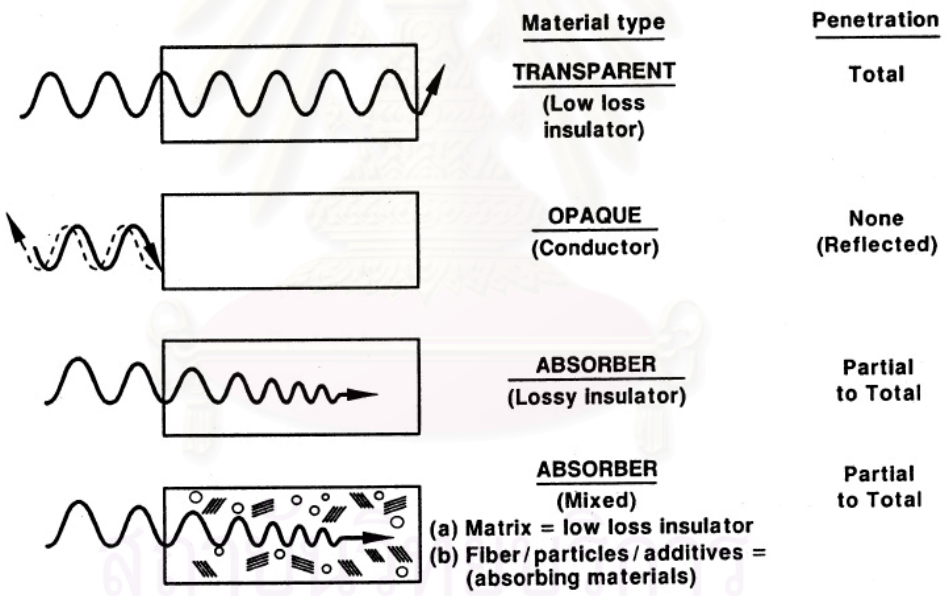

Fig. 2.2 Interaction of microwave with materials [11]

Rahaman [12] defined the permittivity of complex, as shown in equation 2.1

$$\varepsilon_r^* = \varepsilon_r' - j\varepsilon_r'' \tag{2.1}$$

Where ε_r^* is the relative permittivity of the complex, ε' and ε'' are the relative permittivity of the real and imaginary parts of the complex, and $j = \sqrt{-1}$. The dielectric loss or loss tangent, which is used to represent the losses arising from all mechanisms, is defined by

$$\tan\delta = \frac{\varepsilon_r''}{\varepsilon_r'} \tag{2.2}$$

The depth of penetration of the microwave into the material is an important parameter. If the dimension of the material is greater than the depth of penetration, uniform heating cannot occur. The penetration depth, D_p, is defined by

$$D_p \approx \frac{c}{10f(\varepsilon_r')^{1/2}\tan\delta} \tag{2.3}$$

where c is the speed of light and f is the frequency. During microwave radiation, ε_r' and $\tan\delta$ change with temperature and knowing of these changes is important for controlling microwave sintering.

To solve the problem of inefficient microwave heating at lower temperature, the materials are sometimes heated to T_c by conventional heating, then following by microwave heating at higher temperature. Another approach to enhance the heating is partially coating the internal surfaces of a refractory cavity with SiC.

2.2.2. Features of microwave sintering

Since 1970, interest on the application of microwave sintering to oxide ceramics especially for alumina materials has been grown. Microwaves can be used for synthesis, drying, debinding and sintering. Microwave heating is basically different from conventional heating which are typically used for electrical resistance furnaces. The advantage of microwave heating compared to conventional heating is that heat is generated internally by the interaction of the microwave with atoms, ions, and molecules of materials. Furthermore, very high heating rate in excess of 1000°C/min can be achieved. Microwave heating results in lower energy cost, shortened processing time, and significantly enhanced densification [12]. Because of the heat loss from the surface, the thermal gradient obtained by microwave heating is reversed from the conventional heating. That is, the core temperature of microwave-heated sample is higher than the surrounding environment. By combining radiant heating and microwave heating, the thermal gradient in the sample can be substantially reduced [13].

2.2.3. Microwave sintering of Al_2O_3 ceramic

In the 1980s, Meek et al. reported that powders composed of 99.99% pure Al_2O_3 and ZrO_2 were sintered to relative densities of 91.7% and 93.3%, respectively, using 2.45 GHz radiation. Zhipeng Xie et al. [14] reported density variation with holding times at 1500°C under two sintering methods as shown in Fig. 2.3. The microwave sintered sample reached 99.7% theoretical density in a shorter time of 15 min at 1500°C. On the other hand, the conventionally sintered sample reached the same density with longer holding times of 1 hr.

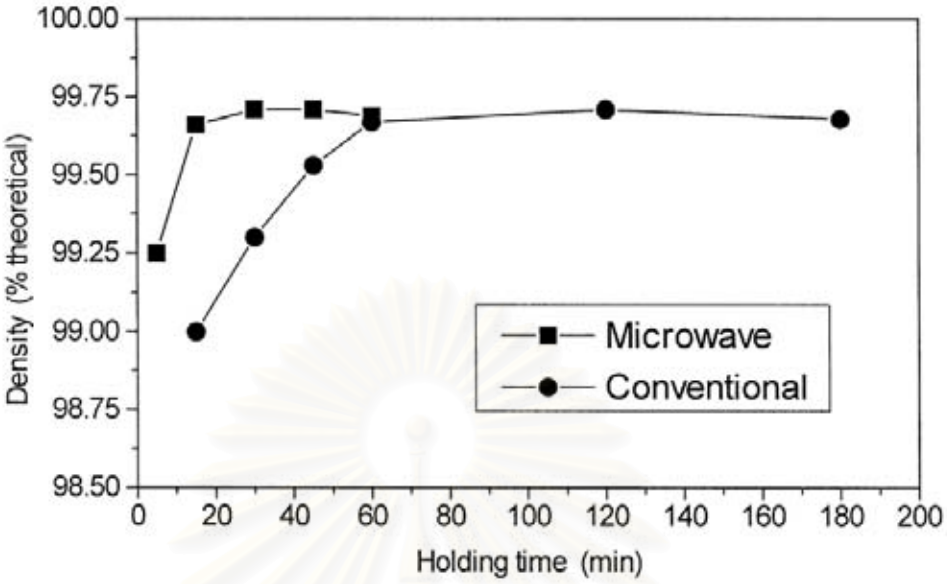

Fig. 2.3 Relationship between final density and holding time at 1500°C for microwave and conventional sintered samples [14]

Janney and Kimrey [15] also observed that Al_2O_3 was densified very rapidly by microwave heating than by conventional heating as shown in Fig. 2.4. They calculated the apparent activation energy for sintering Al_2O_3 by the two processes. Fig. 2.5 shows that the apparent activation energy for microwave sintering which is about one-third of conventional sintering. The large differences in the sintering rate were thought to come from the higher diffusion rates induced by the microwave field.

Tian et al. [16] used microwave heating to fast-fire MgO doped Al_2O_3 (Baikalox CR-30, Baikowski) at 1700°C for 12 min. They reported that grain sizes of Al_2O_3 with 99 and 99.8% theoretical density were 0.8 and 1.9 μm, respectively. They concluded that there was enhanced sintering and they explained that their result came from the early activation of grain boundary and lattice diffusion before surface diffusion could coarsen the microstructure and reduce the driving force for sintering. However, this work was not compared with the conventional one.

Other researchers had reported that the microstructure evolution in microwave sintering produced finer-grained alumina [17,18].

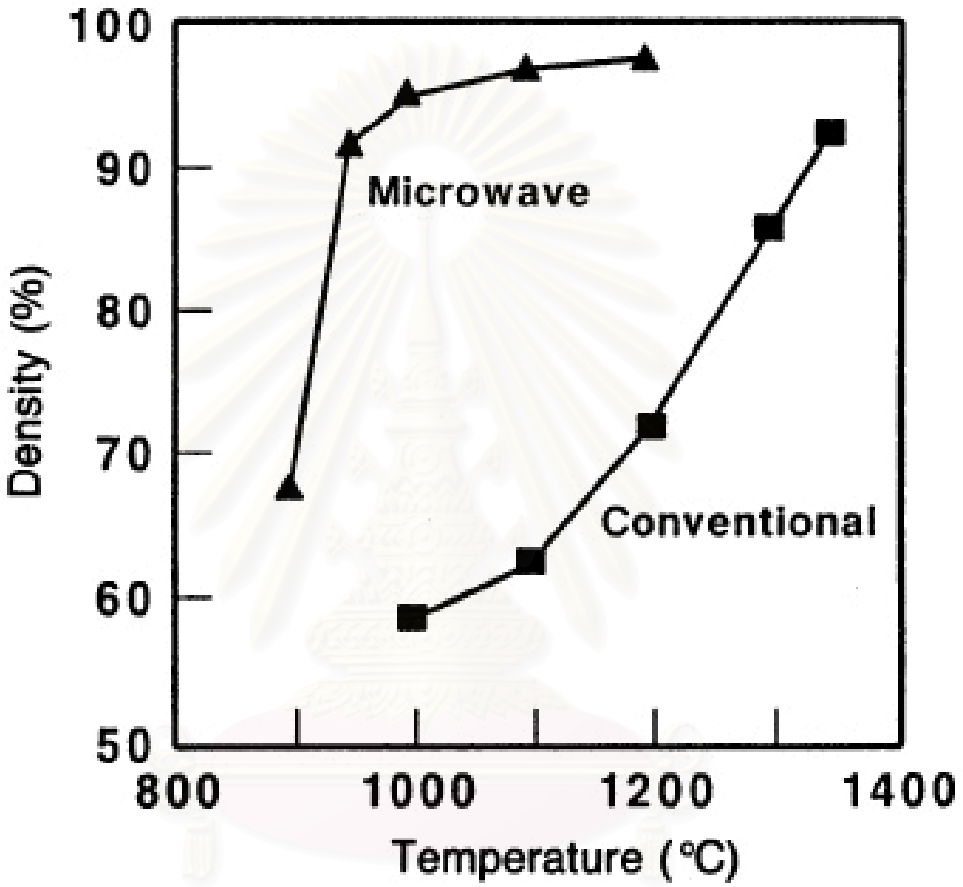

Fig. 2.4 Density versus temperature of microwave (28 GHz) and conventional sintered Al_2O_3 [15]

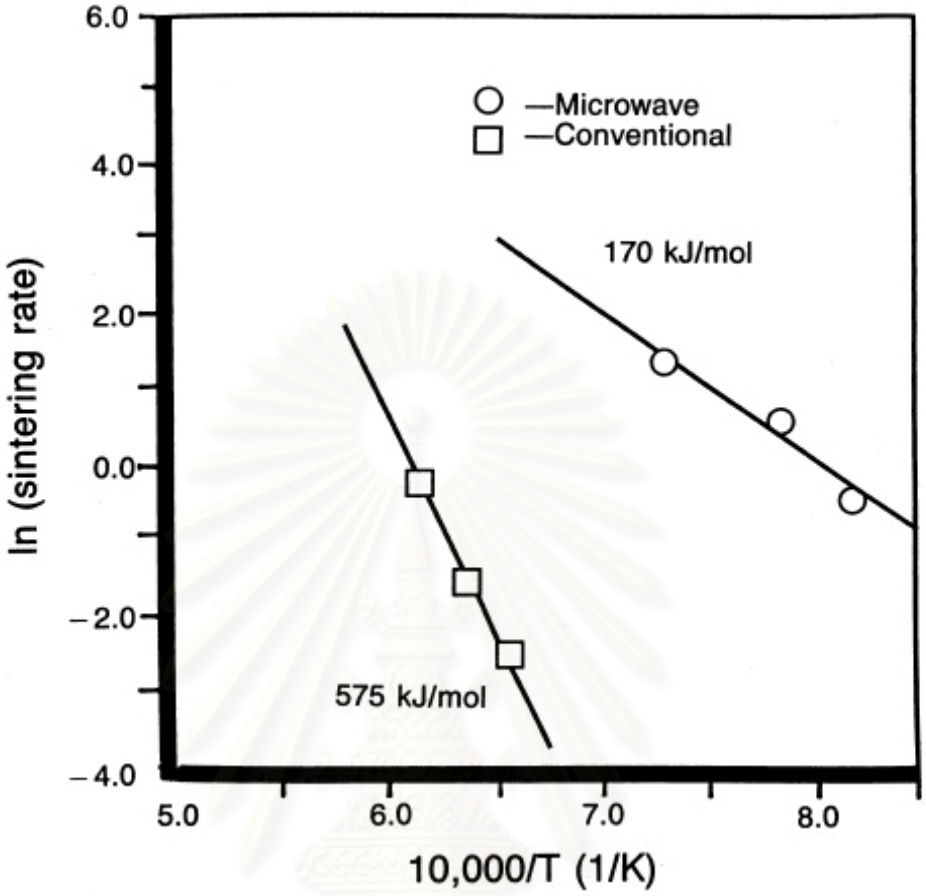

Fig. 2.5 Apparent activation energy for Al_2O_3 sintered by microwave and conventional processes [15]

2.3 Addition of ZrO_2 to Al_2O_3

Grain growth inhibitor is desirable for suppressing the abnormal grain growth during sintering [19]. In order to obtain a high transmittance and mechanical strength, the grain size of alumina needs to be reduced under the submicron level. The effect of doping MgO to alumina has been extensively studied by Coble in 1960 [7]. MgO is one of the major dopants used to reduce grain boundary mobility during sintering [20]. ZrO_2 is also another grain growth inhibitor.

In nature, Zirconium compounds are found as zircon ($ZrSiO_4$) and baddeleyite (ZrO_2) [21]. The average content of zirconia in baddeleyite is 80-90%. Zirconia can be prepared from many processes such as chemical and plasma processes. Zirconia ceramic have been researched for many years. It is an attractive material for high temperature application because of its high melting temperature (2680°C) and excellent corrosion resistance. It shows the polymorphs that are different in crystal structures with the same chemical composition. Three crystallographic forms, monoclinic, tetragonal, and cubic are found for the following temperature ranges [22]

$$\text{Monoclinic} \xrightarrow[1170^{\circ}C]{} \text{Tetragonal} \xrightarrow[2370^{\circ}C]{} \text{Cubic} \xrightarrow[2680^{\circ}C]{} \text{Liquid}$$

The monoclinic phase (m-ZrO_2) is stable at low temperature until 1170°C, and changes to the tetragonal phase (t-ZrO_2). The tetragonal phase is stable up to 2370°C and the cubic phase (c-ZrO_2) of fluorite type becomes stable above this temperature till the melting point of 2680°C [23].

In general, ZrO_2 has been used for reinforcing ceramic products to get high toughness and strength. Furthermore, it is popularly used as grain growth inhibitor in transparent Al_2O_3 ceramic [24]. Andreas Krell et al. [25] used 0.2 wt% ZrO_2 as dopant for transparent Al_2O_3 ceramic. They found that, Al_2O_3 with 0.03 wt% MgO samples are sintered in air (2 h isothermal hold) to densities of ~96% at temperatures of 1240 -1290°C. ZrO_2 doped samples increase this temperature to 1290 -1340°C.

The two Al_2O_3 with and without ZrO_2 were soaked at 1100°C. The transmittance of alumina without ZrO_2 decreased. On the other hand, the transmittance of alumina with ZrO_2 did not change. As a result, ZrO_2 increased the sintering temperature to higher values, however, ZrO_2 prevent additional grain growth in the mean time. Fig. 2.6 shows 30-100 nm small crystallites of ZrO_2 (+3 mol% Y_2O_3) corundum microstructure HIP at 1380°C for 12 h.

Jean-Claude M'Peko et al. [26] reported that ZrO_2 was found to inhibit grain growth of Al_2O_3. The grain size of Al_2O_3 varied from 3.2 to 1.3 μm when ZrO_2 was increased from 0 to 30 vol%. The Al_2O_3 grain size remained constant as ZrO_2 content was further increased. This result is shown in Fig. 2.7

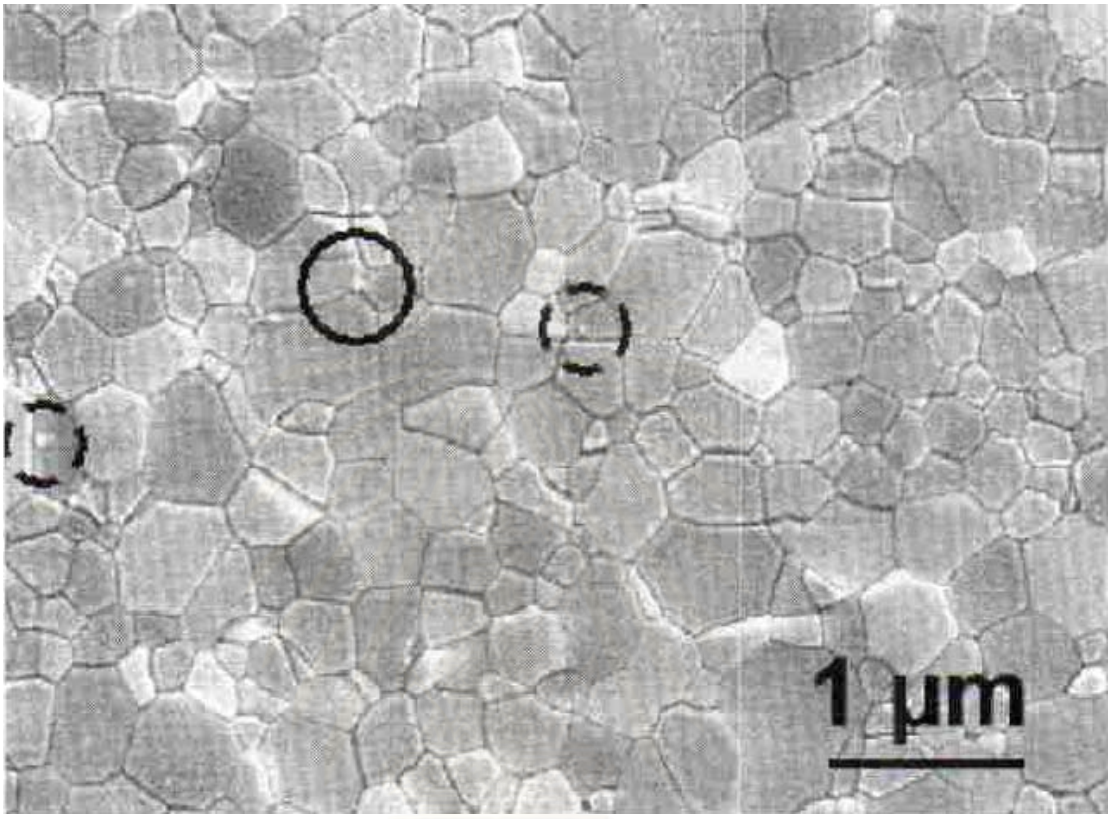

Fig. 2.6 Sintered and sinter-HIP Al_2O_3 (0.41 μm average grain size) doped with ZrO_2 (bright particles). Note the different positions of ZrO_2 crystals (solid circle) intergranular and (dashed circles) intragranular.[25]

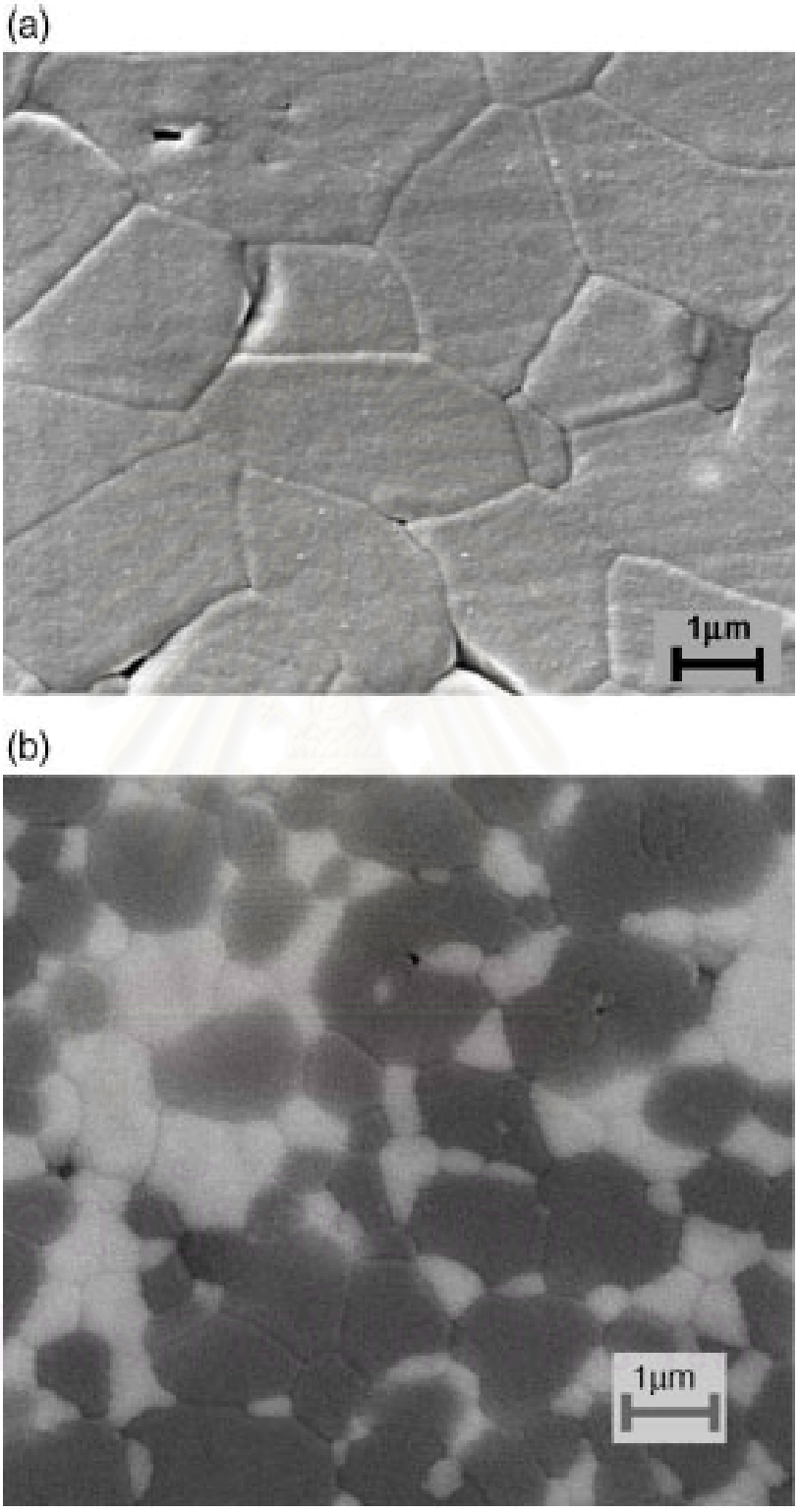

Fig. 2.7 SEM micrographs of (a) pure alumina and (b) a 'conventional' alumina-zirconia composite with 40 vol% of 3YZT, both after sintering at 1600°C for 2 hr.[26]

CHAPTER III

EXPERIMENTAL PROCEDURES

3.1 Raw materials

The starting materials used in this experiment are shown in Table 3.1 [27]. Characterization of alumina powder (TMDA) such as particle size distribution, microstructure, and specific surface area, were observed and reported in Suntorn Tansungnern's thesis (2005) [28].

Table 3.1 Raw materials used in this experiment

Materials	Purity (%)	Manufacturer
Alumina powder (TMDA)	>99.99	Taimei Chemical Co.Ltd., Japan
Zirconia powder (TZ-3YSB)	97.0	Tosoh Corporation
Magnesium Oxide	>99.98	Ube Material Industries, Ltd.
Ethyl Alcohol Absolute	99.8	Carlo Erba Reagents
PVA (MW. 11000-31000)	98.0-98.8	J.T. Baker Inc.

3.2 Sample preparation

3.2.1. Green body specimens

The experimental flowchart is shown in Fig. 3.1. 0.03 wt% MgO based on Al_2O_3 powder was added to Al_2O_3 and were mixed in polypropylene bottle (250 ml) for 3 hr, using ethanol as solvent and Al_2O_3 balls as grinding media. In the study of ZrO_2 addition, the amount of MgO additive was fixed at 0.03 wt% MgO and 0.0, 0.2 and 0.4 wt% of ZrO_2 base on Al_2O_3 powder were blended in ethanol with high purity Al_2O_3 powder. The compositions of various batches are show in Table 3.2.

Mixed slurries were filtrated through sieve #100 and dried at 80°C for 24 hr in oven and then crushed and sieved through the same sieve. PVA 6 wt% solution was added and then crushed and sieved through the same sieve. Green body were pressed into pellets of 25 mm in diameter by biaxial hydraulic press of 20 MPa and followed by Cold Isostatic Press (Dr.CIP, KOBELCO) of 200 MPa.

Table 3.2 Compositions of Alumina powder with MgO and ZrO_2

Composition	Add MgO (wt%)	Add ZrO_2 (wt%)
A	0.03	0.0
B	0.03	0.2
C	0.03	0.4

3.2.2. Sintering

Conventional sintering was performed at temperatures ranging from 1300 to 1500°C for 2 hr with heating rate of 10°C/min in air atmosphere (Box furnace, Linberg Asherille, Nc., U.S.A.).

Microwave sintering was carried out using a small batch type furnace (TAKASAGO INDUSTRY.CO.LTD). The specification of the furnace is shown in Table 3.3 and the photos are shown in Fig. 3.2. Microwave sintering was performed at temperatures ranging from 1250 to 1400°C for 0.5 to 2 hr with heating rates of 10, 30, and 50°C/min in air atmosphere.

Table 3.3 Specification of a small batch type furnace used in this experiment

Manufacturer	TAKASAGO INDUSTRY CO., LTD
Type	MWK-B-6.0
Atmosphere	Air
Firing temperature	1250°C-1600°C
Power of micro-wave (2.45 GHz)	6 kW (1.5 kW × 4)
Furnace dimension	1,620 W × 1,710 H (mm)
Inside furnace dimension	300 W × 3000 H (mm)

3.2.3. Sinter-HIP

Sinter-HIP was performed by Hot Isostatic Press (Dr.HIP, KOBELCO) at 1250 to 1300°C for 0.5 to 1 hr with heating rate of 10°C/min and the pressure of 150 MPa in Ar atmosphere. The sintered specimens, which reached >95% theoretical density, were selected for applying HIP and subsequently polished.

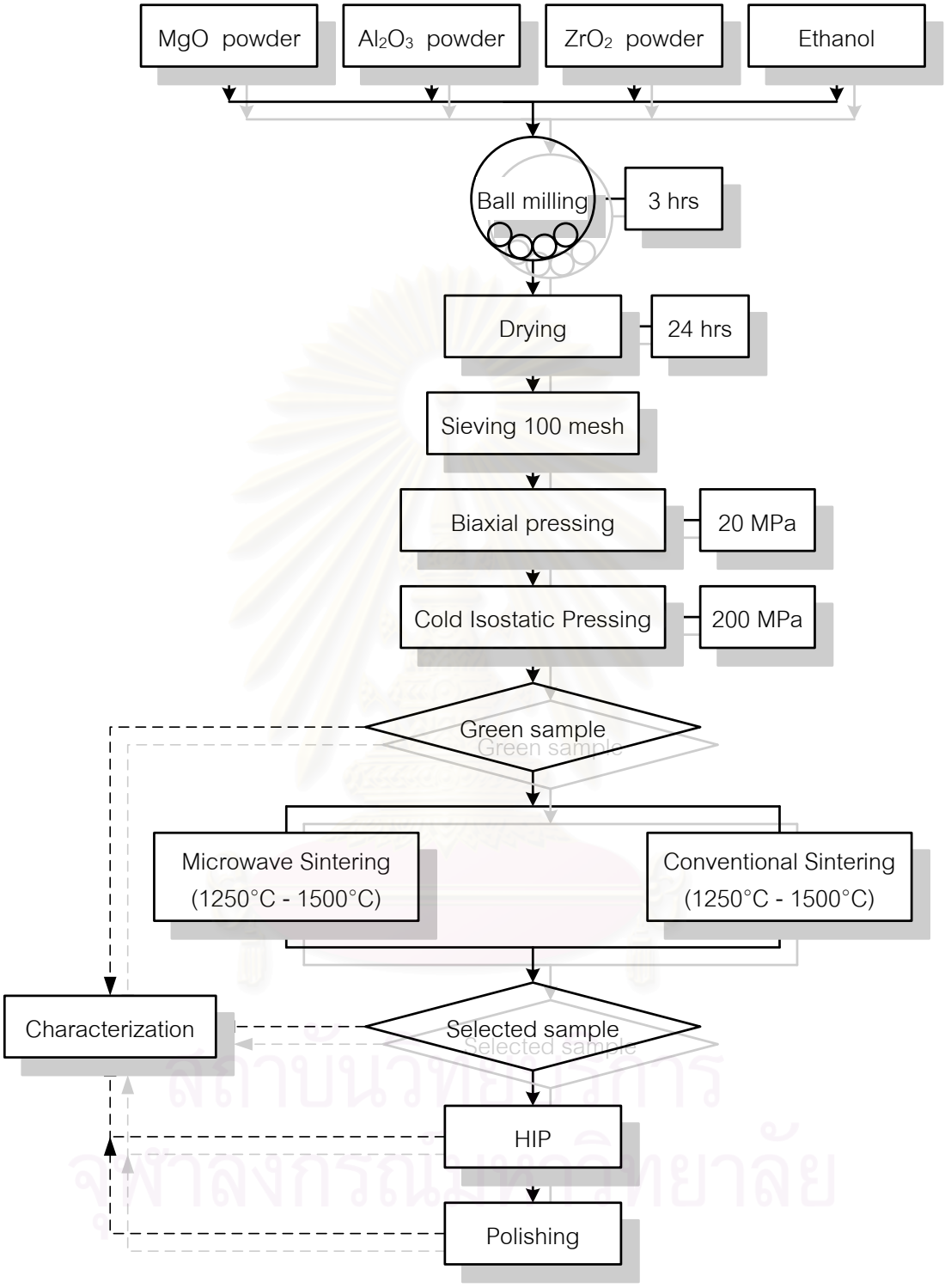

Fig. 3.1 Flowchart of samples preparation process

Fig. 3.2 Microwave furnace used in this experiment.

3.3 Characterization

3.3.1. Characterization of green specimens

The flowchart of sample characterization is shown in Fig. 3.1. The diameter and thickness of green specimens were measured using vernier caliper and the bulk density was calculated by the equation (3.1).

$$\text{Bulk density } (\rho) = \frac{M}{V} \quad (3.1)$$

Where M is the mass of green pellet and V is the volume of green pellet.

3.3.2. Characterization of sintered specimens

The sintered densities were measured by the Archimedes method with an immersion medium of water and the relative densities were calculated with respect to the theoretical density of α-Al_2O_3 (3.98 g/cm^3).

The microstructures of the specimens were observed by scanning electron microscope, SEM (JEOL JSM-6400 model). The specimens were sectioned to a small area for easier polishing. The sectioning operation was performed using diamond blade. The sectioned specimen was mounted in cast resin. The specimens were polished with SiC abrasive paper grit number 240 300 400 and 600 followed by diamond paste (1 μm). Before observing by SEM, the specimens were thermally etched at the temperatures below the sintering temperatures. The specimens sintered at low (<1350°C) and high (>1350°C) sintering temperatures were thermally etched at 20°C and 50°C lower than the sintering temperature for 1 hr, respectively.

The average grain sizes of Al_2O_3 specimens, before and after HIP, were measured by the intercept length method following ASTM standard (E112-96) [29]. The transmittance (%) of specimens after HIP was measured by a double beam automatic recording spectrophotometer UV/VIS spectrophotometer (Perkin Elmer, Lambda 35). The wavelengths of beam were in the range of 200-1100 nm. Before measuring the transmittance (%), the specimens were ground and polished to the thickness of 0.8 mm (BIWAGIMA GIKEN and MEITO GIKEN) at Japanese companies.

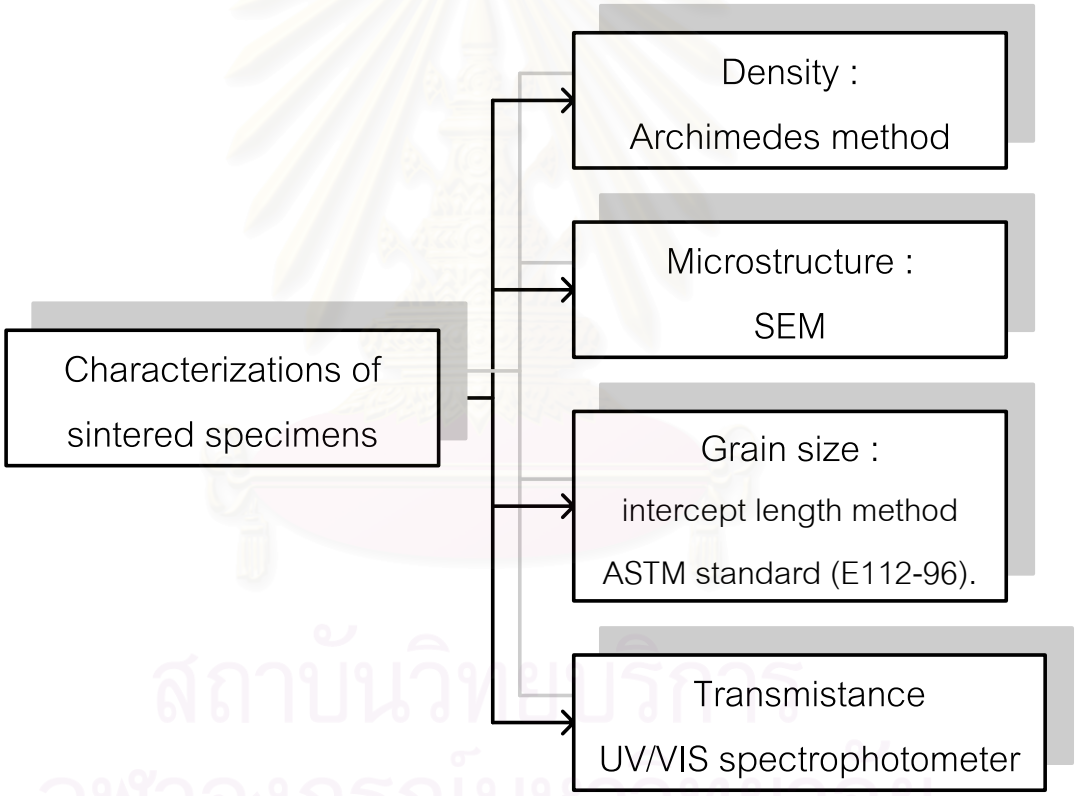

Fig. 3.3 Flowchart of characterizations of sintered specimen

CHAPTER IV

RESULTS AND DISCUSSIONS

4.1 Characterization of green specimens

If the density of green specimen is too low, the high sintered density can not be obtained. For this reason, preparation of green body is very important. To achieve good transparency, green samples should be high density and in good homogeneity [30]. Fig. 4.1 shows the densities of green specimens. The relative density of dry pressed bodies was about 50% and increased to 55% after CIP. The green density did not change with compositions.

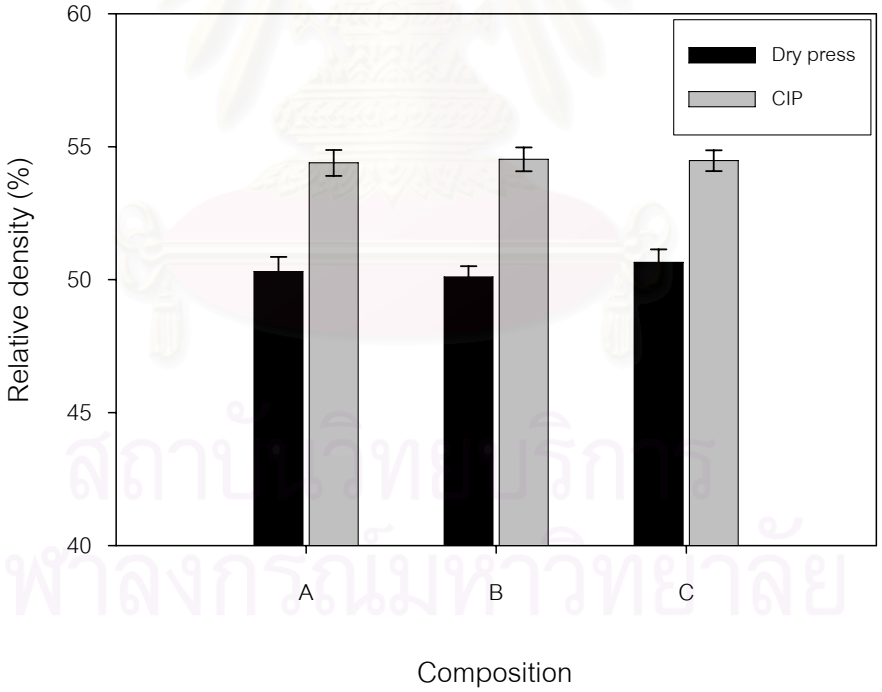

Fig. 4.1 The relative density of green body after biaxial press and followed by CIP.

4.2 Comparison of Microwave sintering and Conventional sintering

4.2.1. Microwave sintering

Fig. 4.2 illustrates the relative density of microwave sintered specimens with different soaking times. All samples were sintered at 1300°C with heating rate of 10°C/min and 50°C/min. A constant power of about 6.5 kW was applied. In this figure the density after sintering was very high and reached 95% of theoretical density in a short period of time (30 min). The relative density gradually increased with longer soaking time. The heating rate did not affect the relative density significantly.

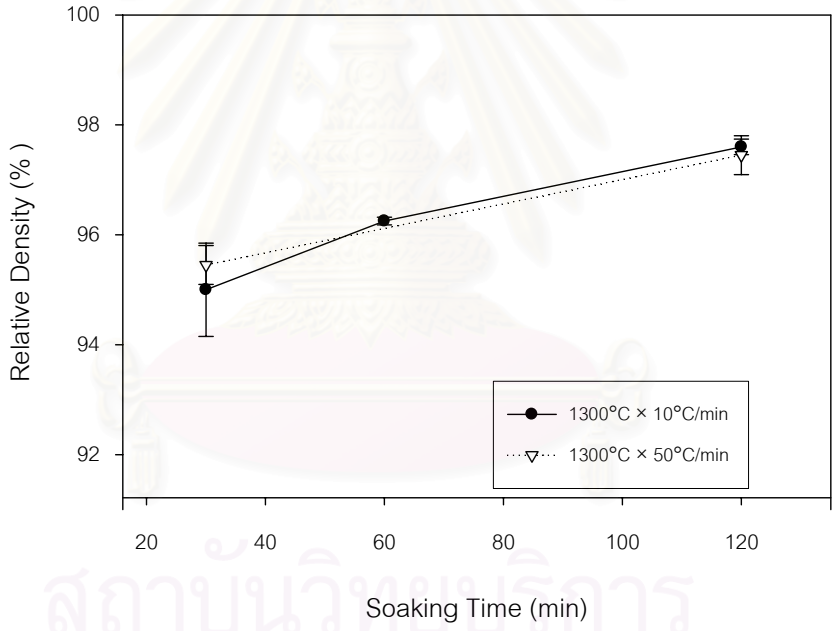

Fig. 4.2 The relative density of microwave sintered Al_2O_3 ceramic sintered at 1300°C as a function of soaking time.

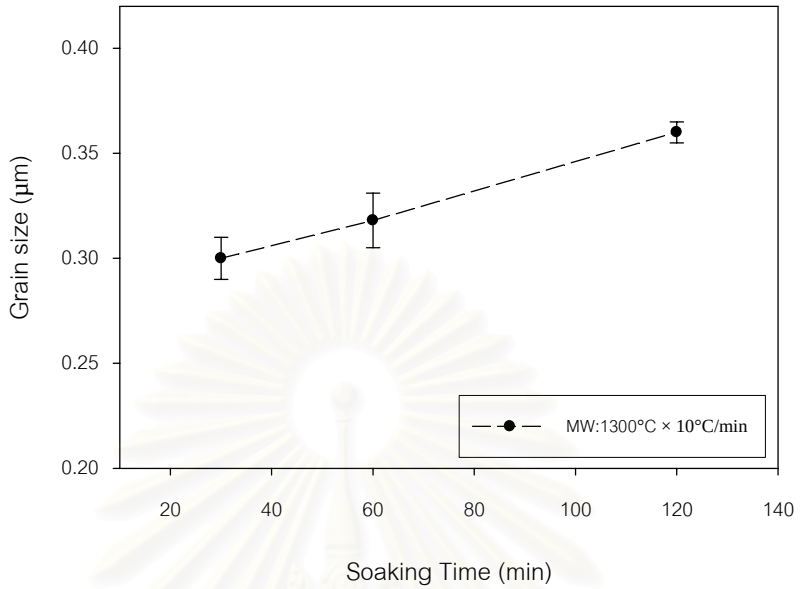

Fig. 4.3 The average grain size of microwave sintered Al_2O_3 ceramic sintered at 1300°C as a function of soaking time.

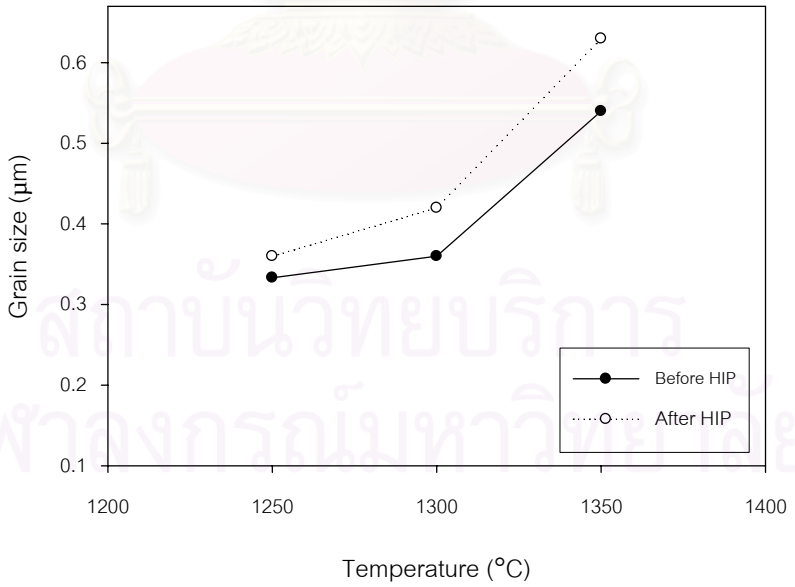

Fig. 4.4 The average grain size of microwave sintered Al_2O_3 ceramic after HIP as a function of sintering temperature. All sample were sintered for 2 hr with a heating rate of 10°C/min.

The average grain size of microwave sintered Al_2O_3 ceramic as a function of soaking time is shown in Fig. 4.3. All samples were sintered at 1300°C with heating rate of 10°C/min. It was found that the average grain size increased with the increase of soaking time. At soaking times of 30 to 120 min, grain size increased from 0.30 to 0.36 μm. The grain size of specimens sintered at different temperatures is shown in Fig. 4.4. The grain size increased with the increase of sintering temperature. The grain size was increased more when the specimen was sintered at 1350°C.

4.2.2. Density of Microwave and conventional sintered specimens

Same batch of mixed powder was sintered by conventional and microwave sintering. The sintering temperatures were at first varied from 1250°C to 1400°C. The optimum sintering temperatures from 1250°C to 1350°C were selected for the following experiment because the density of sintered samples were high enough to get closed pore state (about 95% theoretical density) at 1250°C.

Fig. 4.5 shows the relative density of sintered Al_2O_3 ceramic before and after HIP as a function of sintering temperature. All samples sintered for 2 hr with a heating rate of 10°C/min by microwave and conventional methods. It can be found that microwave sintered sample reached 97% theoretical density at 1275°C. Conventional sintered sample also reached the same density. The microwave sintered samples did not exhibit enhanced densification than conventional sintered.

When the sintered specimens were sinter-HIP, the relative density of samples became very high and close to theoretical density. The relative densities of the specimen sintered at 1275°C and followed by sinter-HIP at 1300°C increased from 96.7 to 99.5 and 96.7 to 99.9% theoretical density using microwave and conventional sintering, respectively. The densities of microwave sintered followed by HIP were a little lower than that of conventional sintered followed by HIP as seen in Fig. 4.5. The reason is not known so far now.

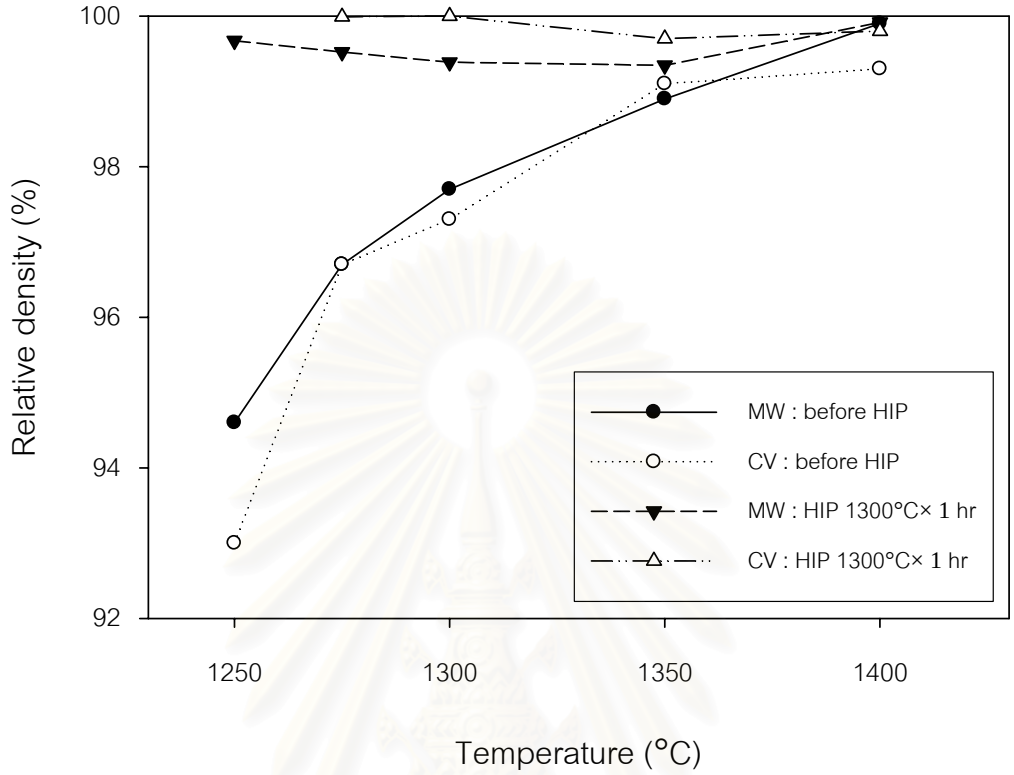

Fig. 4.5 The relative density of sintered Al_2O_3 ceramic before and after HIP as a function of sintering temperatures. All samples were sintered for 2 hr with heating rate of 10°C/min.

4.2.3. Microstructure of microwave and conventional sintered Al_2O_3 specimens

The microstructure of cross sectioned specimens has been studied using SEM. The grain boundaries of polished specimens have been revealed by thermal etching. The average grain sizes of Al_2O_3 specimens, before and after HIP, were measured by the intercept length method following ASTM standard (E112-96). The relation between the average grain size of microwave and conventional sintered Al_2O_3 ceramic as a function of sintering temperatures are shown in Fig. 4.6. All samples were sintered for 2 hr with a heating rate of 10°C/min. It was found that the microwave sintering and conventional sintering showed the similar results. The average grain size increased with increasing the sintering temperatures. The grain size obtained from

microwave heating and conventional heating were a little different. The average grain size of the microwave and conventional sintered specimens at 1300°C were 0.36 and 0.4 μm respectively. Fig. 4.7 shows the transparency and SEM micrographs of sintered specimens. Conventional sintered specimen (a) shows better transparency than microwave sintered specimen (b).

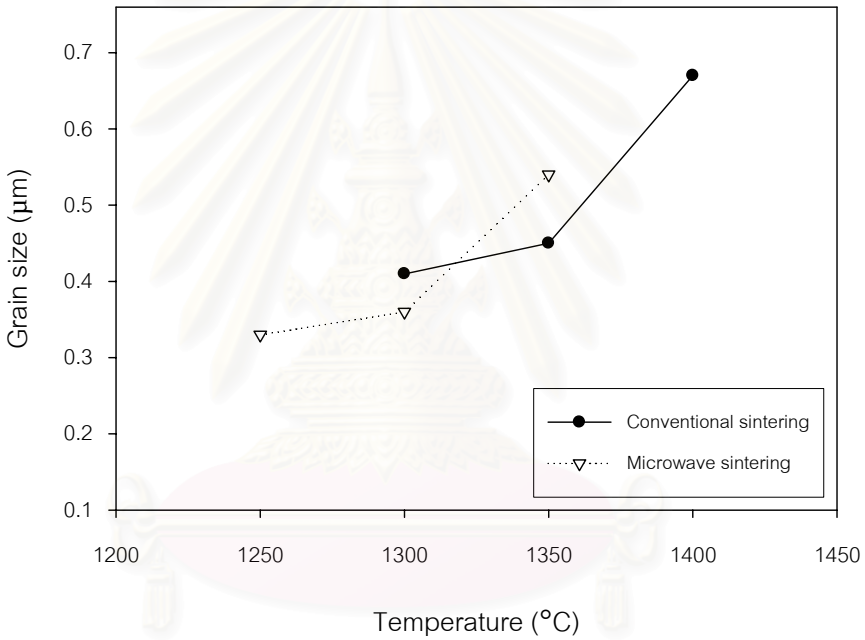

Fig. 4.6 The average grain size of microwave and conventional sintered Al_2O_3 ceramic as a function of sintering temperature. All samples were sintered for 2 hr with heating rate of 10°C/min.

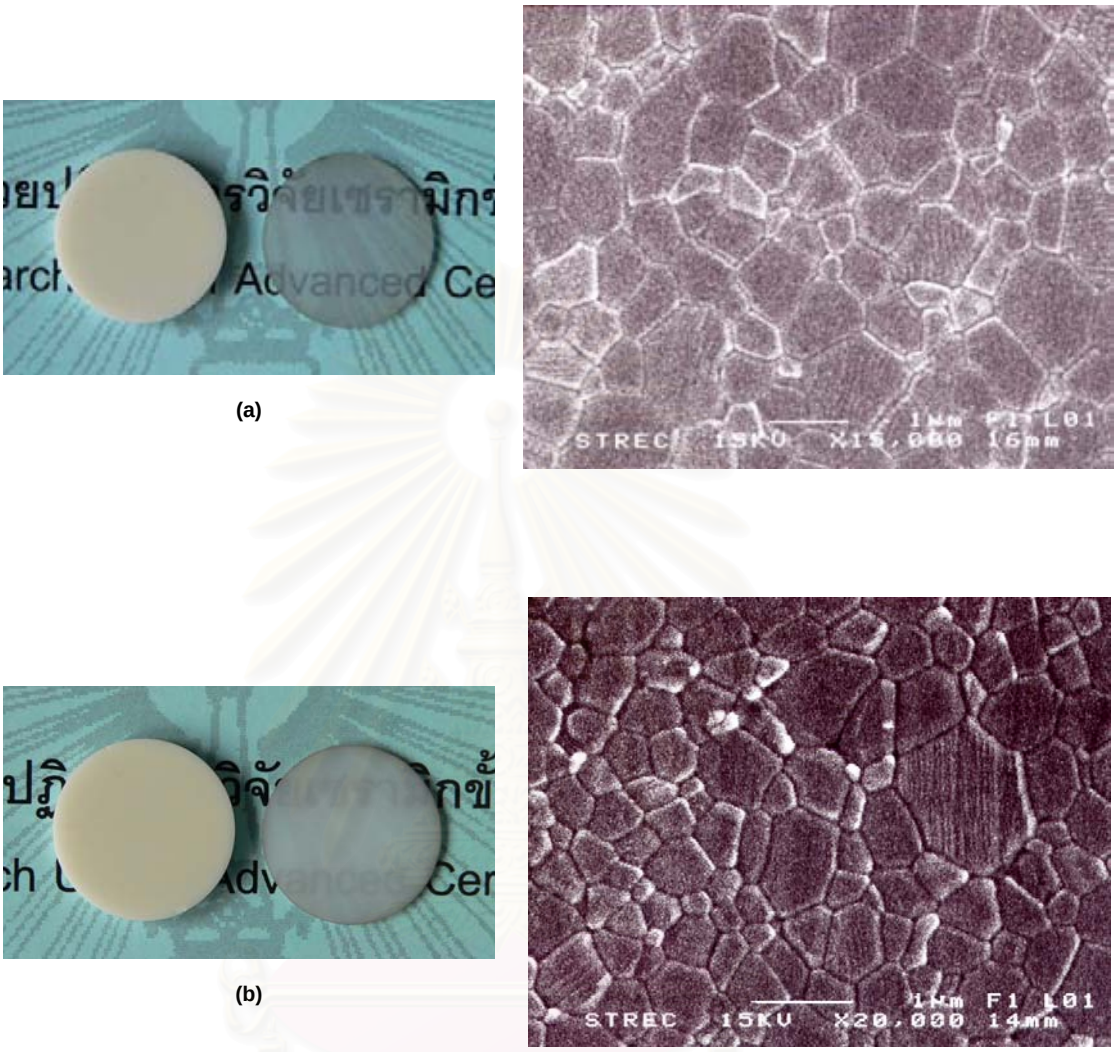

Fig. 4.7 Transparency and SEM micrographs of Al_2O_3 sintered sample (a) CV-6 and (b) MW-4 sinter-HIP at 1300°C for 1 hr with a heating rate of 10°C/min under Ar pressure of 150 MPa.

4.2.4. Grain size distribution

In this work, the light scattering at second phases can be neglected in high purity translucent polycrystalline Al_2O_3 (PCA). Even for MgO-doped PCA, there is no significant effect of MgO on the optical properties of specimens up to 0.03 wt% of MgO content. The scattering of light at the surfaces also can be neglected because the sample surface was smooth. Therefore, grain size and imperfect grain boundary are important for the light scattering of specimens [9].

Grain size distributions of microwave and conventional sinter-HIP specimens are shown in Fig. 4.8. The grain size of microwave sintered specimens is larger than 1.0 μm. On the other hand, the grain sizes of conventional sintered specimen are all less than 1.0 μm. When the average grain size of specimen is larger than 1.0 μm the specimen did not show good transmittance as a result of Mie scattering and refraction [5]. If there are large grains than wavelength, light will be refracted. By the refraction, light scattered and as a result transmittance decreased.

As seen in Fig.4.7, the small grains were apparently found in the microstructure of microwave sintered specimen. The higher amounts of these small grains were significantly distributed all over the microwave sintered specimen. If there are small gaps in grain boundary, reflection may occur. This implies that, lower transmittance of microwave specimens will be due to the wider grain size distribution.

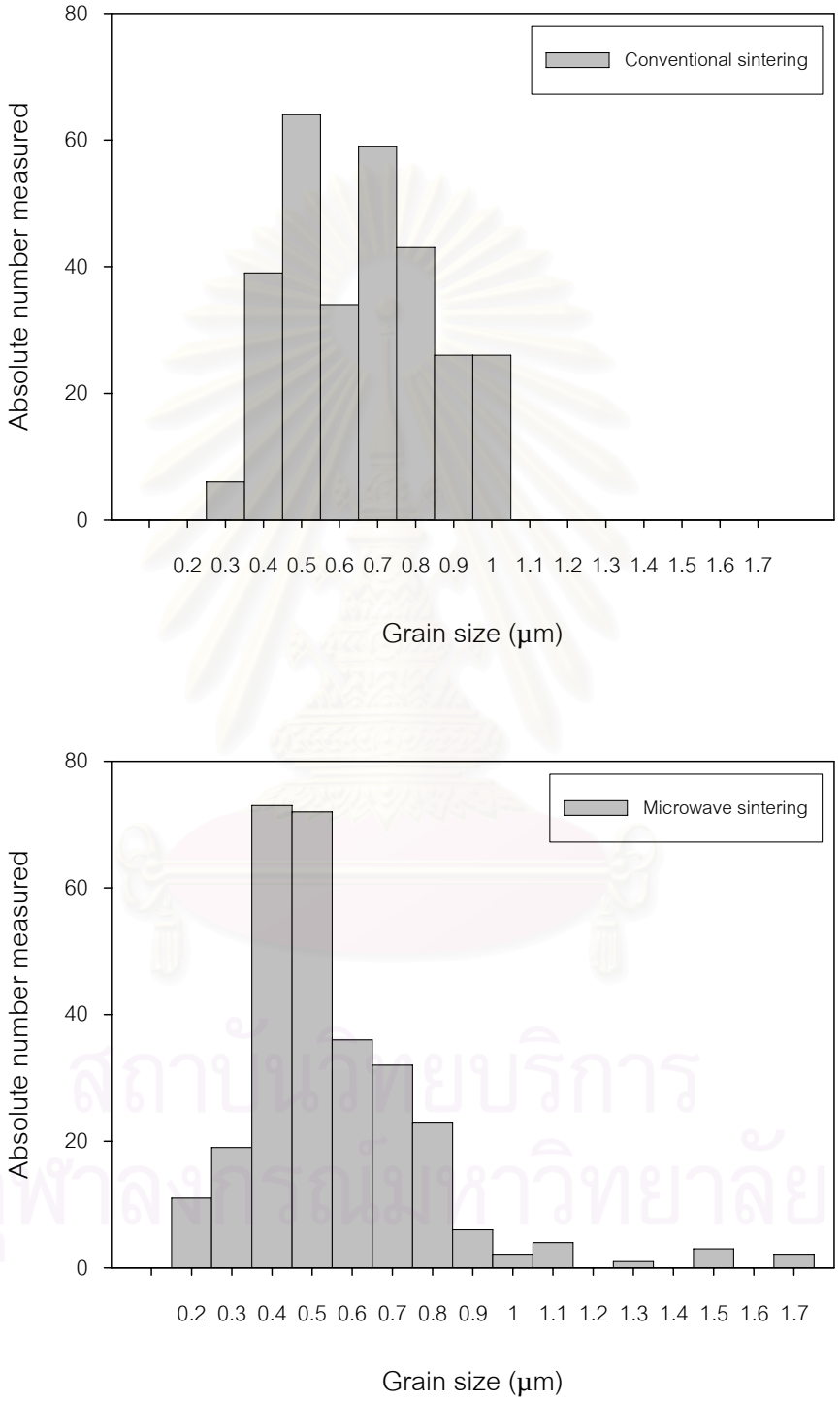

Fig. 4.8 Grain size distribution of microwave and conventional sinter-HIP specimens

4.2.5. Transparency of microwave and conventional sintered specimens

Fig. 4.9 shows the transmittance of microwave and conventional sintered specimens, MW-1, MW-2, MW-3, MW-4 and CV-6 as a function of wavelength. Code of sinter-HIP specimens is shown in Table 4.1. The specimens were sintered at various sintering conditions followed by sinter-HIP at 1300°C for 1 hr with a heating rate of 10°C/min under Ar pressure of 150 MPa. All specimens were ground to 1 mm thick and polished on both side.

The transmittance of CV-6 is better than that of other microwave sintered specimens. The difference might come from the same reason written in section 4.2.3 and 4.2.4. Another reason will be the difference of the density. As seen in Fig. 4.5, the relative density of microwave sintered specimen did not reach 100% of theoretical density. In accordance with the work of Apetz and van Bruggen [9], it was found that small residual porosities results in lower transmittance specimens.

In general, the real in-line transmission (RIT) gradually approaches 86% at long wavelength, whereas the RIT decreases rapidly at shorter wavelength [9]. The transmittance of microwave sintered specimens is low. For example, the transmittance of MW-1, MW-2, MW-3 and MW-4, which measured at wavelength of 645 nm were 1.2, 0.2, 5.6, and 3.2, respectively. The transmittance might be depended on grain size and on the amount and size distribution of pores.

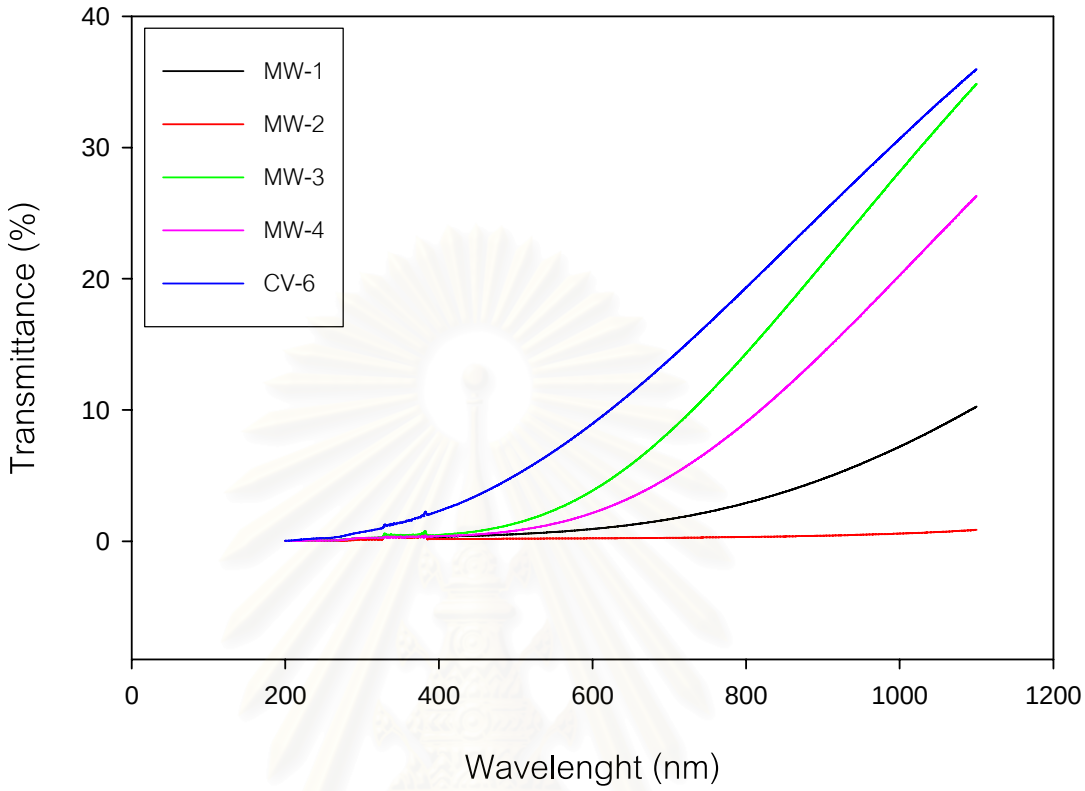

Fig. 4.9 Transmittance (%T) of HIP specimens as a function of wavelength.

Table 4.1 Code of Al_2O_3 sintered-HIP specimens.

Soaking time (hr)	Sintering temperature (°C)			
	1250	1300	1350	1400
0.5	-	MW-3	-	-
2	MW-2	MW-4	CV-6	MW-1

4.3 Effects of soaking time of conventional sintering and HIP condition

4.3.1. Density of sintered specimens at the sintering temperature of 1300°C and 1350°C

In this work, effects of soaking time of conventional sintering and HIP conditions on the microstructure and transparency were studied. Soaking time was changed in the range of 0.5 to 2 hr at 1300°C and 1350°C. The HIP conditions were 1250°C ×1 hr × 150 MPa, 1300°C ×0.5 hr × 150 MPa, and 1300°C ×1 hr × 150 MPa.

Fig. 4.10 shows the relative density of sintered Al_2O_3 ceramic before and after HIP as a function of sintering temperature. All samples were sintered at 1300°C with a heating rate of 10°C/min. Bulk density of sintered samples was 93 and 96% of the theoretical density for 1 and 2 hr soaking, and reached 97.0 and 99.5% of theoretical density after HIP. Bulk density after HIP was not so much affected by the HIP conditions, temperature and soaking time. The low bulk density of 97% means that specimen sintered at 1300°C for 1 hr includes some amount of open pore.

Fig. 4.11 also shows the result of bulk density for the specimen sintered at 1350°C for 0.5, 1, and 2 hr. It was founded that the bulk density after HIP was also no clear difference between HIP conditions and sintering conditions. From these data seen in Fig. 4.10 and Fig. 4.11, bulk density easily increase to almost theoretical value after HIP.

Fig. 4.12 shows the appearance of as sintered and as HIP specimens. HIP specimens show translucency. However, transparency was not good, because the surface of as sintered specimen was rough. The color of specimen also changed. The cause may be the difference of atmosphere between sintering and HIP.

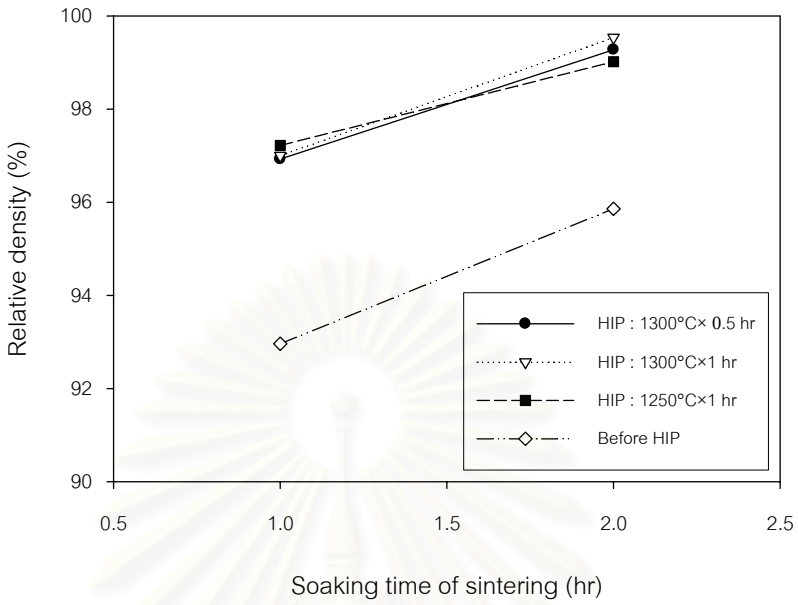

Fig. 4.10 The relative density of sintered Al_2O_3 ceramic before and after HIP as a function of soaking time. All samples were sintered at 1300°C with a heating rate of 10°C/min.

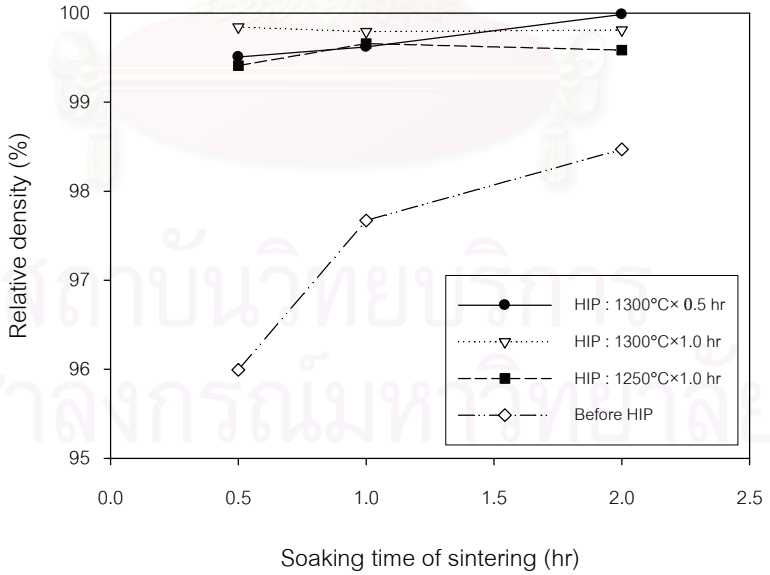

Fig. 4.11 The relative density of sintered Al_2O_3 ceramic before and after HIP as a function of soaking time. All samples were sintered at 1350°C with a heating rate of 10°C/min.

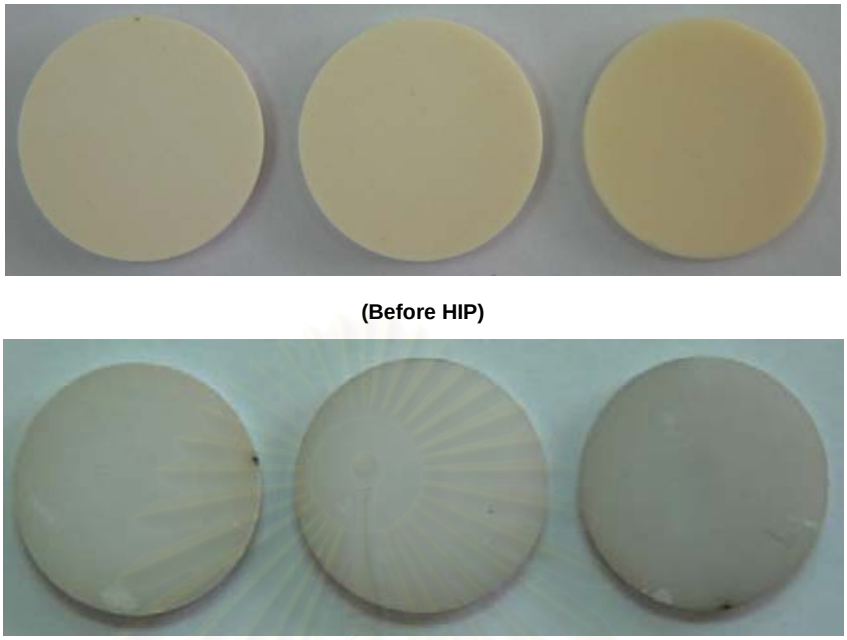

Fig. 4.12 Appearance of Al_2O_3 specimens before and after HIP, sintered at 1300°C for 0.5 hr (left), 1 hr (center) and 2 hr (right).

4.3.2. Microstructure of specimens

Fig. 4.13 shows the grain size of sintered Al_2O_3 ceramic before and after HIP. All samples sintered at 1350°C with heating rate of 10°C/min. Grain size of sintered specimens increased with increasing the soaking time. After sinter-HIP, grain growth occurred. The grain growth during sinter-HIP is also proportional to the sintering temperatures and soaking time qualitatively.

Fig. 4.14 shows SEM micrographs of sintered Al_2O_3 ceramic at various HIP conditions and soaking time. Fig. 4.15 shows SEM micrograph of the specimen sintered at 1350°C ×0.5 hr. In the specimen before HIP, there are many small particles. These small particles decreased by HIP as seen in Fig. 4.14. Comparing CV-1, CV-3, CV-5 with CV-2, CV-4, CV-6, respectively, not only the average grain size increased as seen in Fig. 4.13, but also the largest grain size increased as seen in Fig. 4.14.

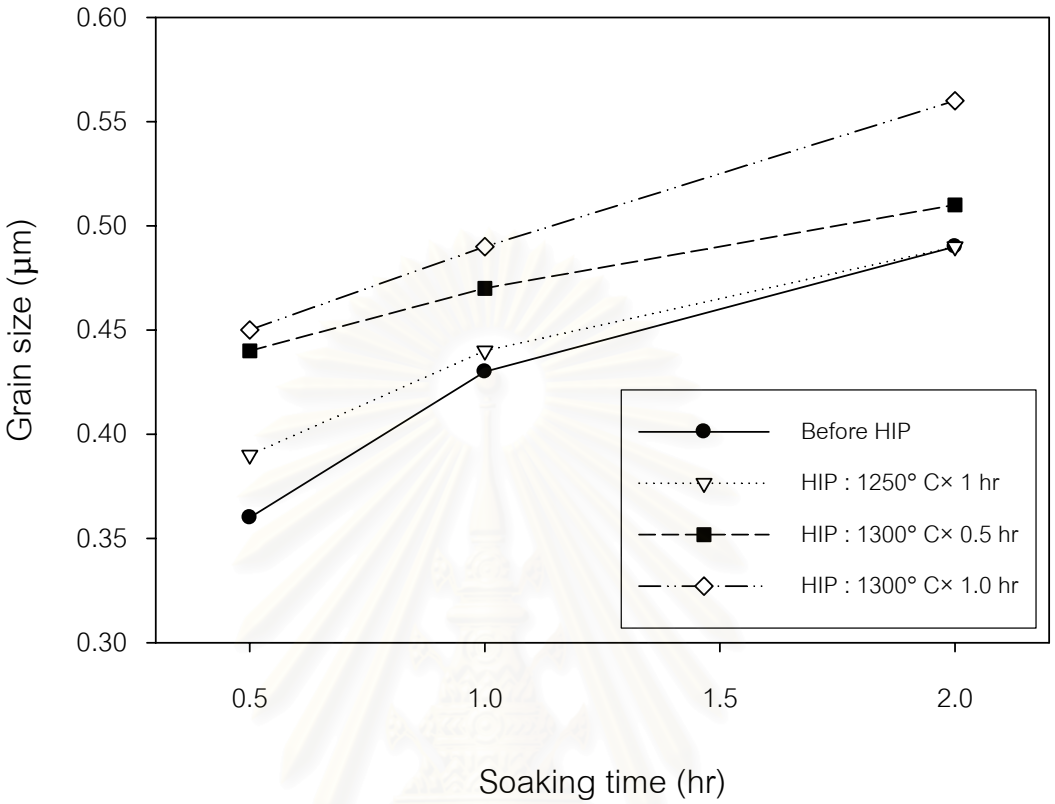

Fig. 4.13 The average grain size of sintered Al_2O_3 ceramic before and after HIP as a function of soaking time. All samples were sintered at 1350°C with a heating rate of 10°C/min.

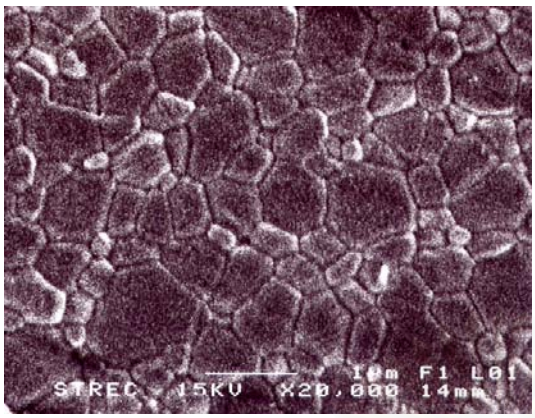

CV-1

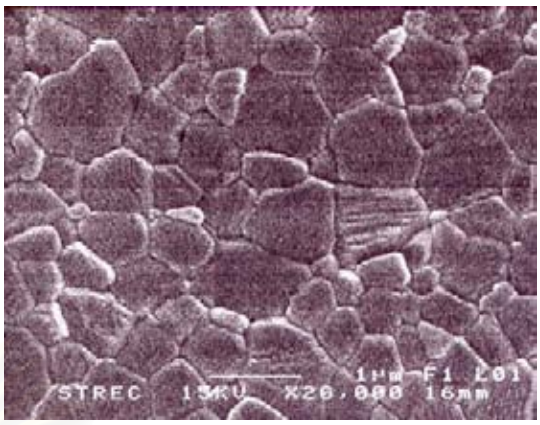

CV-2

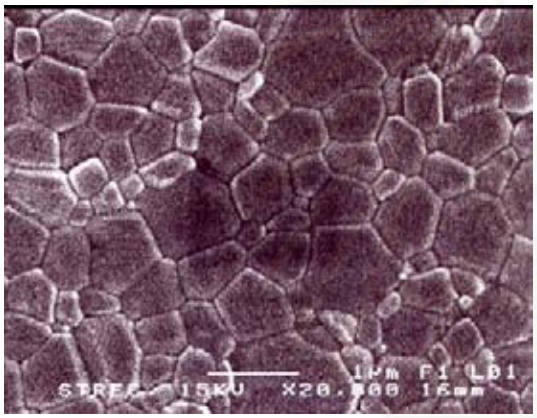

CV-3

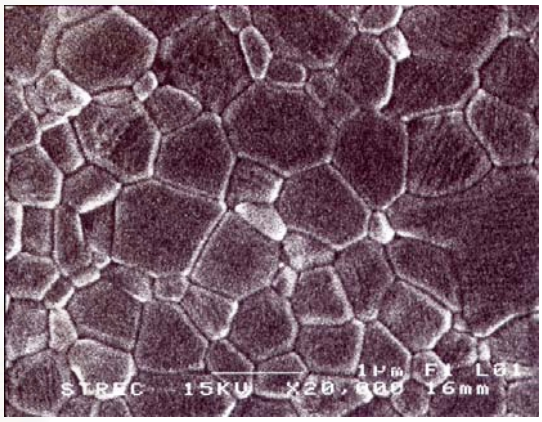

CV-4

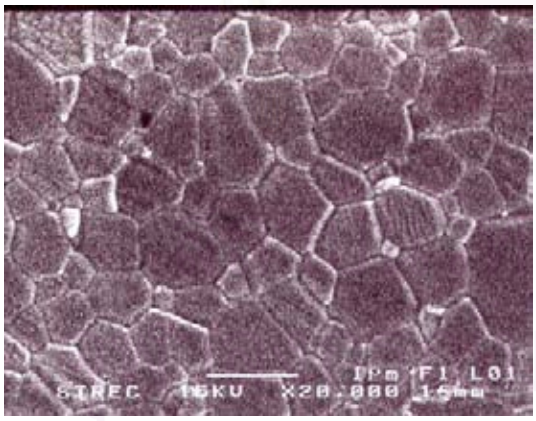

CV-5

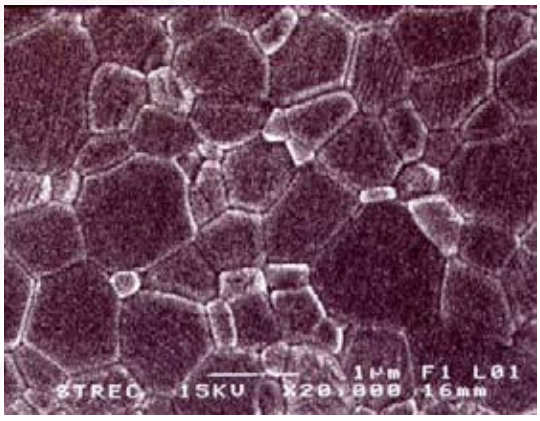

CV-6

Fig. 4.14 SEM micrographs of sintered Al_2O_3 ceramic at various HIP conditions and soaking time.

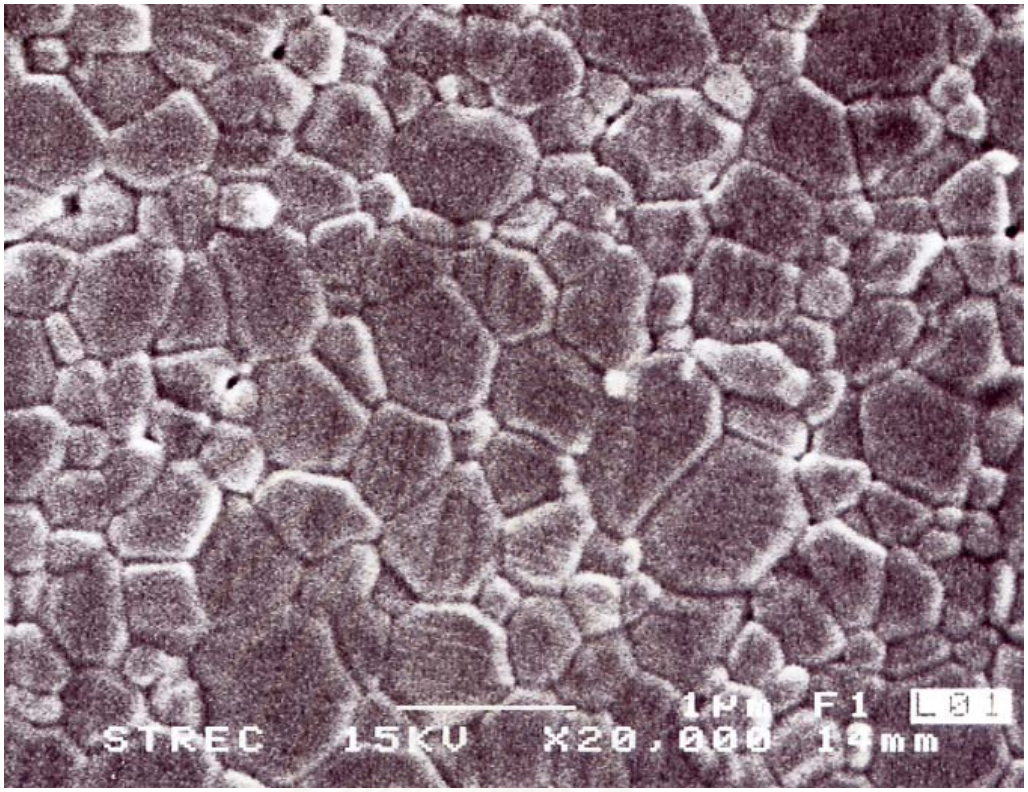

(Before HIP)

Fig. 4.15 SEM micrographs of sintered Al_2O_3 ceramic before HIP.

4.3.3. Transparency of sintered specimens at 1300°C and 1350°C

Fig. 4.16 shows the transparency of sinter-HIP Al_2O_3 ceramic, specimens CV-1-CV-6, as a function of wavelength. All samples were ground to 1 mm thick and polished on both side. Code of conventional sinter-HIP specimens is shown in Table 4.2.

The transmittance of CV-1, CV-2, CV-3, CV-4, CV-5, and CV-6, measured at wavelength of 645 nm, were 22, 13, 24, 21, 26 and 11, respectively. The transmittance of each sintered specimen also increased when the wavelength of the incident light was increased. It was found that CV-1, CV-3 and CV-5 showed the better transparency than CV-2, CV-4 and CV-6, respectively. As discussed in section 4.3.2, the good transparency is the result of smaller average grain size. Normally the light transmission of transparent poly-crystalline alumina increased with increasing wavelength. When wavelength of light is longer than the grains size of specimen, it passes through specimen without or few scattering at grain boundaries. On the other hand, if wavelength of light is shorter than grains size of specimens, it can not pass through specimen, but refracts, reflects and easily scatters. Therefore, when wavelength becomes shorter, transparency decreases [9].

CV-5 showed the best result. The picture is shown in Fig. 4.17. This implies that short soaking time of 0.5 hr is sufficient time for sintering at 1350°C and sinter-HIP at 1300°C. For that reason, the best HIP condition will be used in the future work.

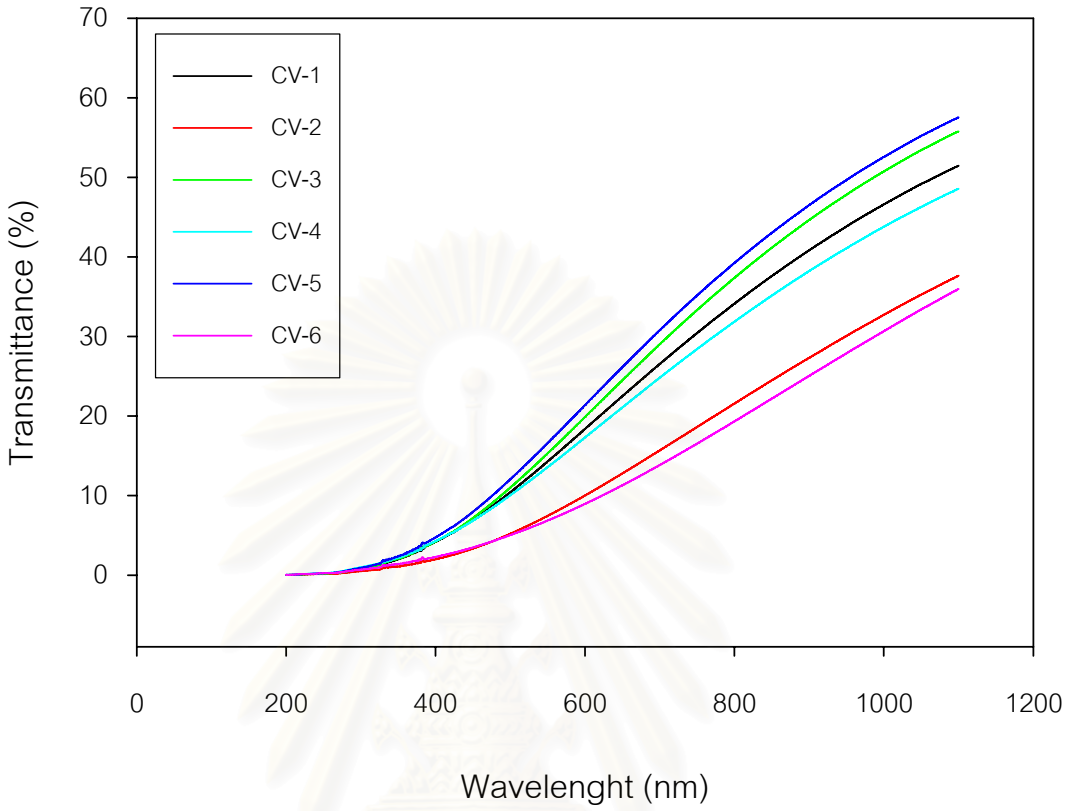

Fig. 4.16 Transmittance (%T) of conventional sintered specimens as function of wavelength. All samples were HIP at 1300°C ×1 hr × 150 MPa under Ar atmosphere.

Table 4.2 Code of Al_2O_3 conventional sintered-HIP specimens.

Sintering condition (°C×hr)	HIP condition (°C×hr)		
	1250×1	1300×0.5	1300×1
1350×0.5	CV-1	CV-3	CV-5
1350×2	CV-2	CV-4	CV-6

Fig. 4.17 Transparency of conventional sintered Al_2O_3 specimen (CV-5)

4.4 Effect of ZrO_2 addition

In order to achieve the microstructure of Al_2O_3 ceramic with homogeneous and submicron grain size, it is necessary to add small amount of MgO. The following work was carried out using 0.03 wt% MgO as a sintering aid for all of Al_2O_3 samples. Various content of ZrO_2 was also added as grain growth inhibitor. Zero (composition A), 0.2 (composition B), and 0.4 (composition C) wt% of ZrO_2 (TZ-3YSB) were blended in ethanol with high purity Al_2O_3 powder (TMDA).

4.4.1. Relative density of sintered specimens

Fig. 4.18 shows the relative density of conventional sintered composition A, B, and C as a function of sintering temperature soaked for 2 hr with a heating rate of 10°C/min. At the low temperature region of 1300 - 1400°C, the bulk density of composition B and C were lower than that of composition A. The small amount of ZrO_2 as 0.2 and 0.4 wt% obviously inhibited the densification. When sintering temperature increased to 1450°C, the density of all composition reached 99% of theoretical density.

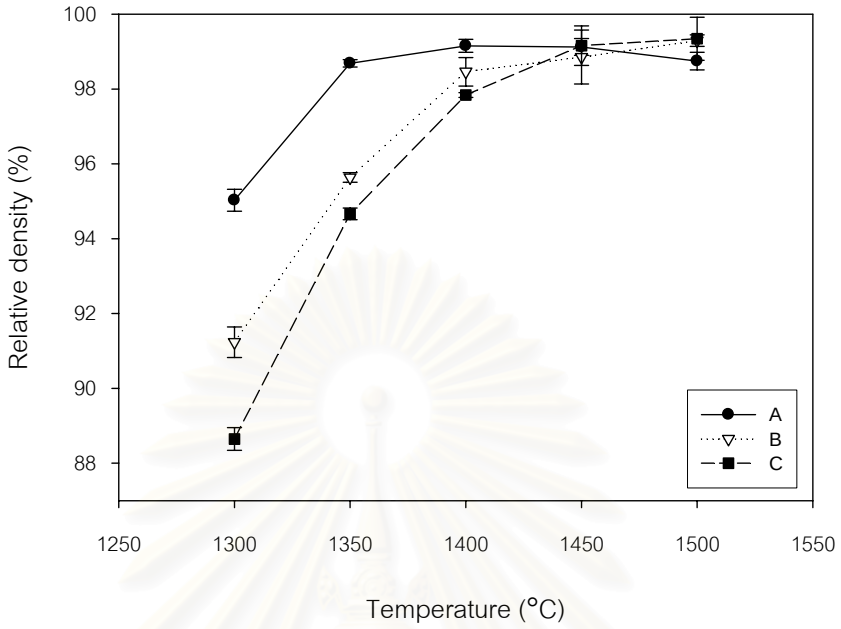

Fig. 4.18 The relative density of conventional sintered Al_2O_3 ceramic as a function of sintering temperature, soaked for 2 hr with a heating rate of 10°C/min.

4.4.2. Microstructure of sintered Al_2O_3 specimens

The average grain sizes of sintered specimens are plotted in Fig. 4.19. It can be noted that the average grain size increased with the increase of sintering temperature, but decreased with the increase of ZrO_2. The average grain size of Al_2O_3 increased slowly below 1450°C, but increased rapidly over 1450°C. The average grain size of composition A, B, and C, which were sintered at 1300°C are 0.54, 0.39, and 0.33 μm, respectively. The average grain size of composition A sintered at 1300°C is almost equal with that of composition B and C sintered at 1400°C. When the relative density of B and C reached over 98%, the grain size grew to 0.5 μm. Therefore, it was difficult to sinter the composition with ZrO_2 to high density with small grain size.

The SEM photographs of composition A, B, and C sintered at 1400 and 1500°C for 2 hr are shown in Fig. 4.20. Grain size distribution of composition B and C samples are not uniform and including many very small grains. On the other hand,

specimens sintered at 1500°C show grain growth. Generally, the average grain size should be less than 0.5 μm when sintered at 1350°C as shown in Fig. 4.13 and distribution of grain size should be narrow as shown in Fig. 4.14. In this sense, ZrO_2 added composition B and C do not realize the ideal microstructure.

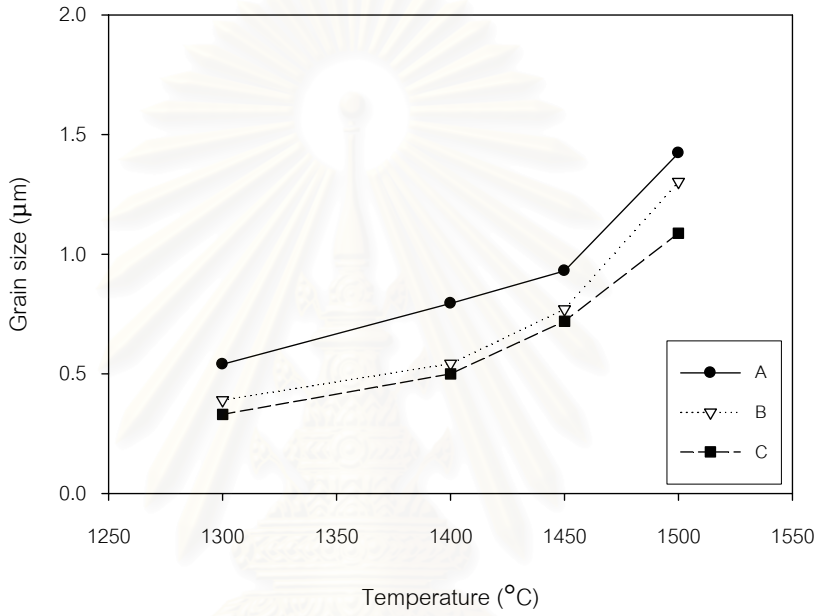

Fig. 4.19 Grain sizes of conventional sintered Al_2O_3 ceramic as a function of sintering temperature, soaked for 2 hr with a heating rate of 10°C/min

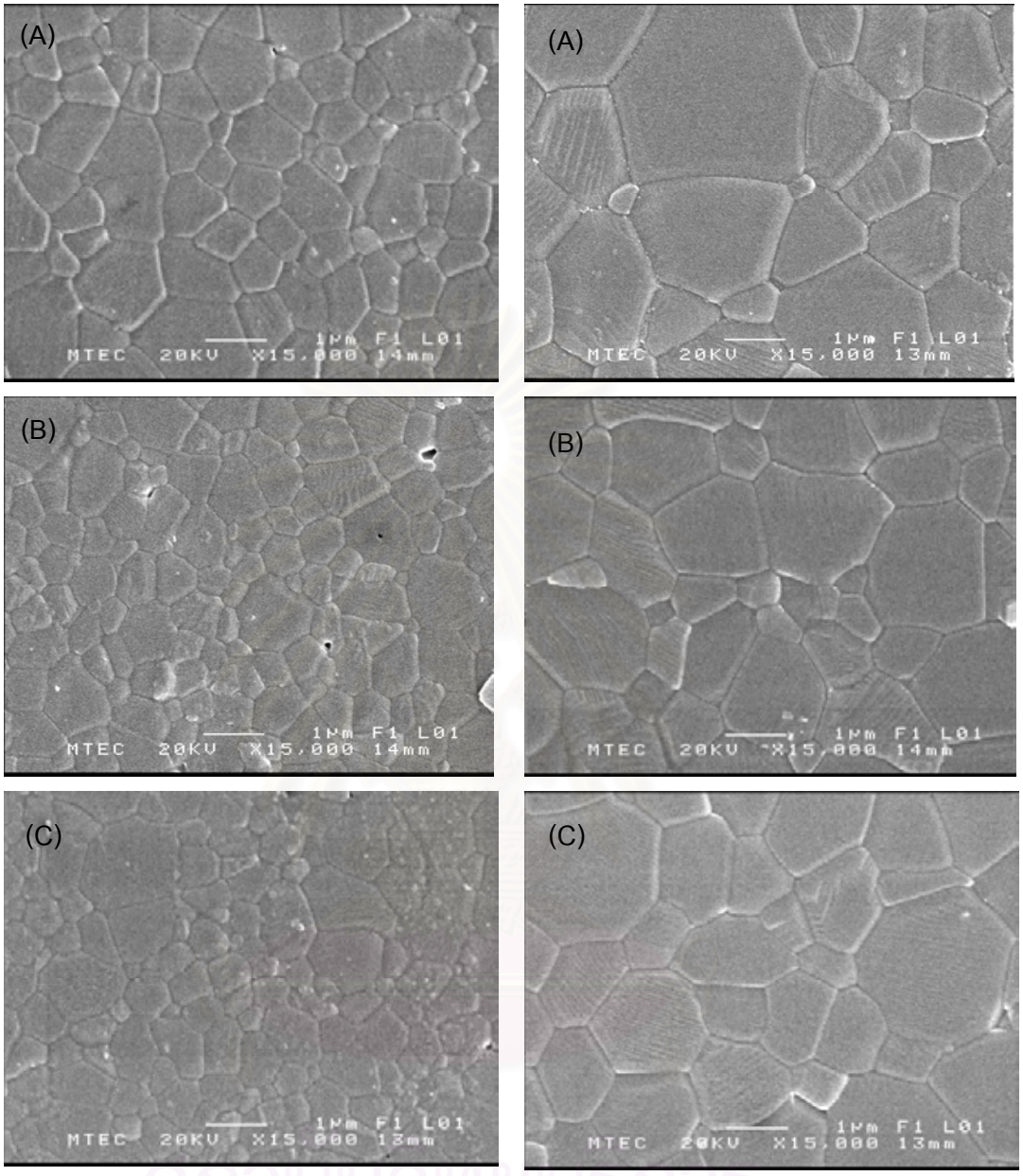

Sintering Temperature 1400 ° C Sintering Temperature 1500 ° C

Fig. 4.20 The microstructure of the composition A, B and C specimens sintered at 1400 and 1500°C for 2 hr with a heating rate of 10°C/min.

4.4.3. Density of sinter-HIP specimens

Fig. 4.21 shows the relative density of HIP specimens, composition A, B, and C as a function of sintering temperature. The specimens were HIP at 1300°C for 1 hr with a heating rate of 10°C/min. From this figure, the relative density after HIP of composition B and C at any sintering temperatures were still lower than composition A and not reached 100% of theoretical density. Therefore, ZrO_2 added specimens were not translucent by observing by naked eye, due to the low relative density even after HIP.

.

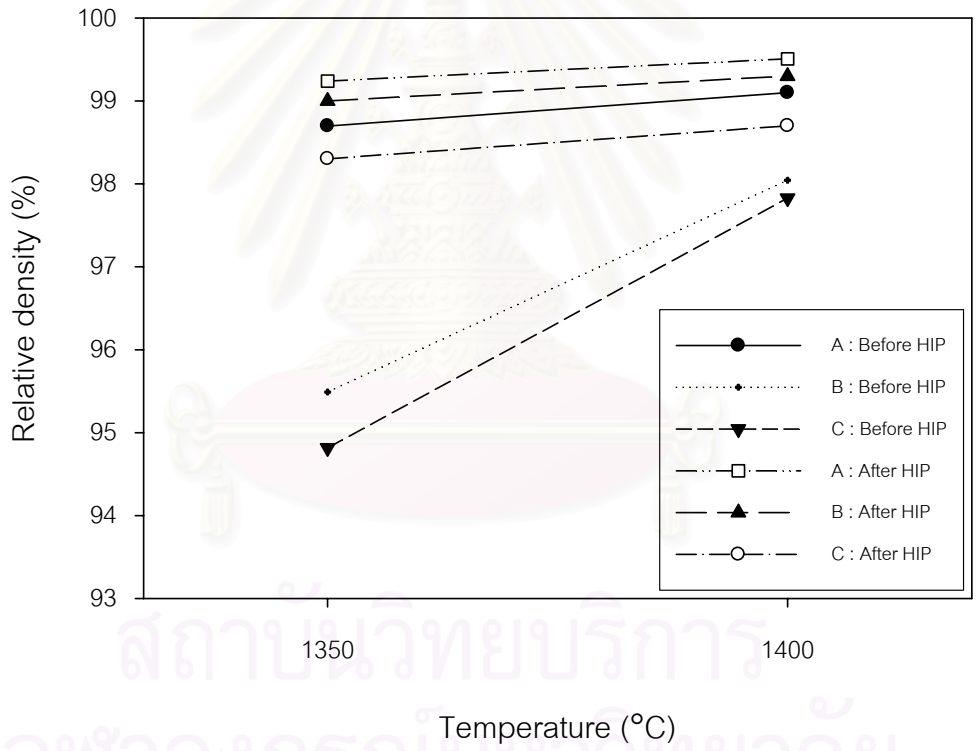

Fig. 4.21 The relative density of HIP specimens as a function of sintering temperature, sinter-HIP at 1300°C for 1 hr with a heating rate of 10°C/min.

4.4.4. Summary on the effect of ZrO_2 addition

When ZrO_2 was added to Al_2O_3 with 0.03 wt% MgO, both of densification and grain growth were disturbed. However, the effect to suppress densification was strong. As a result, Al_2O_3 ceramic with high density and smaller grain size than no ZrO_2 additive composition was not obtained.

CHAPTER V

CONCLUSIONS

In this experiment, effects of microwave sintering and ZrO_2 addition on microstructure and optical transmittance of Al_2O_2 ceramic were studied. The following conclusions have been drawn from this study.

5.1 Microwave sintering

1. Microwave sintering resulted in a fast processing to sinter Al_2O_3 ceramic. It accelerated densification, but did not show the higher density than that of conventional sintering.
2. Average grain size of microwave sintered specimens was a little smaller than that of conventional one. The grain size increased with the increase of sintering temperature.
3. Soaking time is one of the important factors on the grain growth. Short soaking time of 0.5 hr was sufficient for sintering at 1350°C and sinter-HIP at 1300°C.
4. The transmittance of microwave sintered specimens was lower than that of conventional one because of the wider grain size distribution.

5.2 ZrO_2 addition

1. A small amount of ZrO_2 addition, 0. 2-0.4 wt%, inhibited densification and grain growth of ZrO_2 at 1300-1400°C. When sintering temperature increased to 1450°C, the density of all compositions reached to 99% of theoretical density.
2. The grain size of the full density specimen with ZrO_2 was a little larger than that without ZrO_2. Therefore, better optical transmittance was not attained by adding ZrO_2.

CHAPTER VI

FUTURE WORKS

It is well known that vacuum and hydrogen atmosphere during sintering is better to get higher density specimen at lower sintering temperature than conventional air atmosphere sintering.

To increase density of Al_2O_3 specimens at lower sintering temperature, sintering in vacuum and hydrogen atmosphere and suitable HIP condition should be studied.

REFERENCES

[1] Dirk Godlinski, Meinhard Kuntz, and Georg Grathwohl, "Transparent Alumina with Submicrometer Grains by Float Packing and Sintering," J. Am. Ceram.Soc. 85, 10 (2003): 2449-2456.

[2] Zhipeng Xie, Jinlong Yang, and Yong Huang, "Densification and grain growth of alumina by microwave processing," Materials Letters. 37 (1998): 215-220.

[3] Curtis Scott, and Mary Kaliszewski, "Conversion of Polycrystalline Al_2O_3 into Single-Crystal Sapphire by Abnormal Grain Growth," J. Am. Ceram. Soc. 85, 5 (2002): 1275-1280.

[4] M. Adams. Zirconium Oxide, ZrO_2. [online]. Available from: http://www.accuratus.com/zirc.html . [2006, January 9].

[5] Y.T. O, J.B. Koo, K.J. Hong, J.S.Park, and D.C. Shin, "Effect of Grain size on Transmittance and Mechanical Strength of Sintered Alumina," Materials Science and Engineering A 374 (2004): 191-195.

[6] Donald J. Sandstrom, "Armor Anti-Armor Materials by Design," Los Alamos Science Summer. (1989).

[7] Jiping Cheng, Dinesh Agrawal, Yunjin Zhang, and Rustum Roy, "Microwave sintering of transparent alumina," Materials Letters 56 (October 2002): 587-592.

[8] Michel W. Barsoum. Fundamentals of Ceramics. New York : The McGraw-Hill, (1997).

[9] Rolf Apetz, and Michel P.B. van Bruggen, "Transparent Alumina: A Light-Scattering Model," J. Am. Ceram. Soc 86,3 (2003): 480-86.

[10] Yi Fang, Jiping Cheng, and Dinesh K. Agrawal, "Effect of powder reactivity on microwave sintering of alumina," Materials Letters. 58 (2004): 498-501.

[11] W. Sutton, "Microwave Processing of Ceramic Materials," Amer. Ceram. Soc. Bull. 68,2 (1989): 376-386.

[12] M.N. Rahaman, Ceramic Processing and Sintering (New York: Marcel Dekker,Inc, 2003), p.818.

[13] Kristen H.Brosnan, Gary L.Messing, and Dinesh K. Agrawal, "Microwave Sintering of Alumina at 2.45 GHz," J. Am. Ceram. Soc 86,8 (2003): 1307-12.

[14] Zhipeng Xie, Jinlong Yang, and Yong Huang, "Densification and grain growth of alumina by microwave processing," Materials Letters. 37 (1998): 215-220.

[15] M.A. Janney, and H.D. Kimrey, Ceram. Trans., Ceram. Powder. Sci 1 (1988) 919.

[16] Y.L Tian, D. L. Johnson, and M. E. Brodwin, "Ultrafine Microstructure of Al_2O_3 Produced by Microwave Sintering," Ceramic Transsactions,Vol.1 (1988): 925-932.

[17] Zhipeng Xie, Jinlong Yang, Xiangdong Huang and Yong Huang, "Microwave Processing and Properties of Ceramics with Different Dielectric Loss," Journal of the European Ceramic Society. 19 (1999): 381-387.

[18] Jiping Cheng, Dinesh Agrawal, Rustum Roy, and P.S. Jayan, "Continuous microwave sintering of alumina abrasive grits," Journal of Materials Processing Technology. 108 (2000): 26-29.

[19] Kamol Panmaung, "Development of Alumina-Zirconia Composite for Milling Ball," (Master's thesis, Ceramic Technology, Faculty of Science, Chulalongkorn University, 2003),

[20] G. C. WEI, "Grain Growth and Sintering of Translucent Polycrystalline Alumina," Journal of the Ceramic Society of Japan, Supplement 112-1, PacRim5 Issue. 112,3 (2004): S179-S182.

[21] R. Stevens, Zirconia and Zirconia ceramics: Chemical Zirconia second edition, pp.9-10. Leeds: Magnesium Electron.

[22] Michel Barsoum, Fundamentals of Ceramics: One Component Systems, (Singapore: McGraw-HILL,1997) pp. 267-269.

[23] Khanthima Hemra, "High Strength Materials: Alumina-Zirconia Composite Using Low Cost Raw Powder," (Master's thesis, Ceramic Technology, Faculty of Science, Chulalongkorn University, 2003),

[24] Xin Guo, Wilfried Sigle, Jurgen Fleig, and Joachim Maier, "Role of Space Charge in The Grain boundary Blocking Effect in Doped Zirconia," Solid State Ionics. 154-155 (2002): 551-561.

[25] Andreas Krell, Paul Blank, Hongwei Ma, and Thomas Hutzler, "Transparent Sintered Corundum with High Hardness and Strength," J.Am.Ceram. Soc 86,1 (2003): 12-18.

[26] Jean-Claude M'Peko, Deusdedit L. Spavieri Jr., Charled L. da Silve, Carlos A. Fortulan, Dulcina P.F. de Souza, and Milton F. de Souza, "Electrical Properties of Zirconia-Alumina Composites," Solid State Ionics 156 (2003): 59-69.

[27] Tosoh Corporation: The Chemistry of Innovation. Zirconia Powders Easy Modability Grades. [online]. Available from : http://www.tosoh.com/Products/es+basic2_grades.htm. [2006, December 23].

[28] Soontorn Tansungnoen, "Development of Transparent Nano-Crystalline Alumina Ceramic: Effects of Forming and Sintering Condition," (Master's thesis, Ceramic Technology, Faculty of Science, Chulalongkorn University, 2005),

[29] ASTM E112-96. Standard Test Methods for Determining Average Grain Size. ASTM International. 2004.

[30] Andreas Krell, and Jens Klimke, "Effects of the Homigeneity of Particle Coordination on Solid-State Sintering of Transparent Alumina," J. Am. Ceram. Soc 89,6 (2006): 1985-1992.

APPENDICES

APPENDIX A

Preliminary experiment results

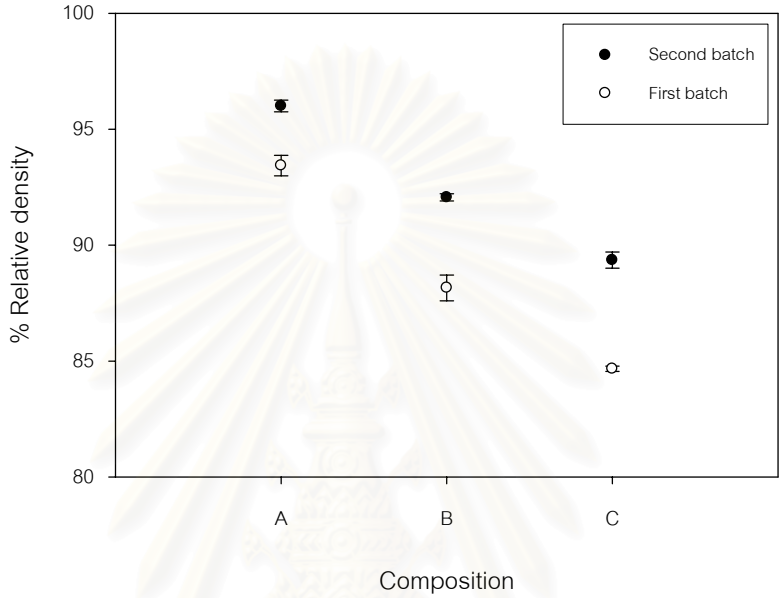

Effect of calcinations on sintered density specimen

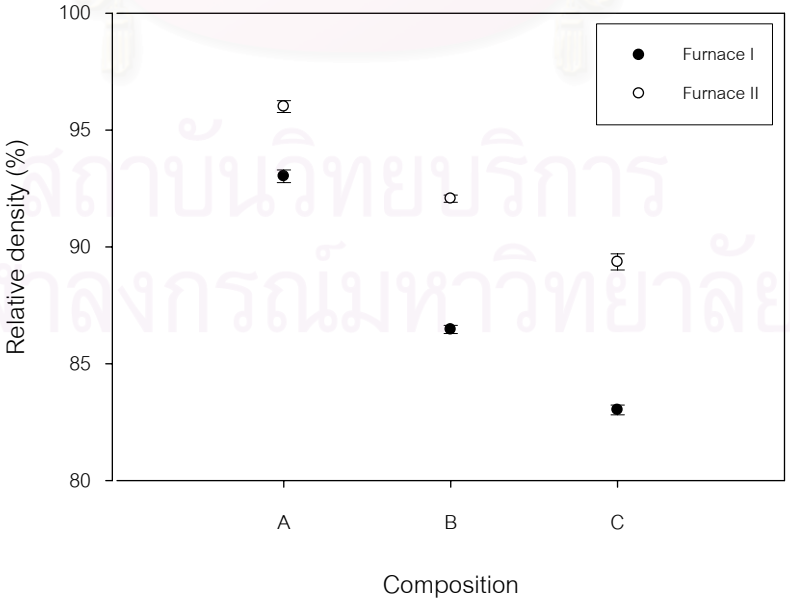

Effect of conventional furnace on sintered density specimen

APPENDIX B

Density of green body, which prepared by biaxial press method.

Sample number	Mass (g)	Radial (cm)	Thickness (cm)	Volume (cm^3)	Bulk Density (g/cm^3)	Relative Density (%)
1	2.73	1.28	0.27	1.38	1.98	54.4
2	2.79	1.28	0.28	1.43	1.95	53.6
3	2.74	1.28	0.28	1.40	1.95	54.8
4	2.74	1.28	0.28	1.43	1.92	54.4
5	2.74	1.28	0.28	1.43	1.91	53.6
6	2.74	1.28	0.28	1.43	1.92	53.9
7	2.72	1.28	0.28	1.43	1.90	55.1
8	2.74	1.28	0.28	1.43	1.92	55.1
9	2.72	1.28	0.28	1.43	1.90	54.6
10	2.75	1.28	0.29	1.46	1.89	54.3
11	2.73	1.28	0.28	1.43	1.91	54.9
12	2.74	1.28	0.28	1.43	1.92	54.0
13	2.81	1.28	0.29	1.46	1.93	54.7
14	2.76	1.28	0.28	1.43	1.93	54.1
15	2.78	1.28	0.28	1.43	1.94	54.4
16	2.75	1.28	0.28	1.43	1.93	54.4
17	2.75	1.28	0.28	1.43	1.92	54.4
18	2.75	1.28	0.28	1.43	1.92	53.6
				AVG.	1.92	54.8
				S.D.	0.02	0.52

APPENDIX C

Green body density of composition A, B and C prepared by biaxial press method and followed by CIP.

Composition A number	Mass (g)	Radial (cm)	Thickness (cm)	Volume (cm^3)	Bulk Density (g/cm^3)	Relative Density (%)
1	1.86	0.96	0.30	0.86	2.16	54.4
2	1.83	0.96	0.30	0.86	2.13	53.6
3	1.85	0.97	0.29	0.85	2.18	54.8
4	1.84	0.97	0.29	0.85	2.17	54.4
5	1.85	0.96	0.30	0.87	2.13	53.6
6	1.81	0.96	0.30	0.85	2.14	53.9
7	1.84	0.96	0.29	0.84	2.19	55.1
8	1.82	0.96	0.29	0.83	2.19	55.1
9	1.83	0.96	0.29	0.84	2.17	54.6
10	1.81	0.96	0.29	0.84	2.16	54.3
11	1.83	0.96	0.29	0.84	2.18	54.9
12	1.87	0.96	0.30	0.87	2.15	54.0
13	1.86	0.96	0.30	0.85	2.18	54.7
14	1.84	0.96	0.30	0.85	2.15	54.1
15	1.85	0.96	0.30	0.85	2.17	54.4
				AVG.	2.16	54.4
				S.D.	0.02	0.49

Composition B number	Mass (g)	Radial (cm)	Thickness (cm)	Volume (cm^3)	Bulk Density (g/cm^3)	Relative Density (%)
1	1.86	0.96	0.30	0.87	2.14	53.8
2	1.86	0.96	0.29	0.84	2.21	55.5
3	1.86	0.97	0.30	0.86	2.16	54.1
4	1.84	0.97	0.29	0.85	2.17	54.4
5	1.84	0.96	0.29	0.84	2.18	54.6
6	1.85	0.97	0.29	0.85	2.18	54.8
7	1.86	0.97	0.29	0.85	2.19	55.0
8	1.83	0.96	0.29	0.84	2.18	54.6
9	1.82	0.96	0.29	0.84	2.16	54.2
10	1.83	0.97	0.29	0.85	2.16	54.3
11	1.83	0.96	0.29	0.84	2.17	54.5
12	1.83	0.96	0.30	0.85	2.15	54.0
13	1.85	0.96	0.30	0.85	2.17	54.4
14	1.84	0.96	0.29	0.84	2.20	55.1
15	1.84	0.97	0.29	0.85	2.17	54.5
				AVG.	2.17	54.5
				S.D.	0.02	0.45

Composition C number	Mass (g)	Radial (cm)	Thickness (cm)	Volume (cm^3)	Bulk Density (g/cm^3)	Relative Density (%)
1	1.84	0.96	0.29	0.84	2.18	54.6
2	1.83	0.96	0.30	0.85	2.15	53.9
3	1.82	0.96	0.29	0.83	2.19	54.8
4	1.82	0.96	0.29	0.83	2.20	55.3
5	1.82	0.96	0.29	0.84	2.17	54.3
6	1.83	0.97	0.29	0.85	2.16	54.1
7	1.86	0.96	0.30	0.86	2.15	53.9
8	1.83	0.96	0.29	0.84	2.16	54.3
9	1.85	0.96	0.30	0.85	2.16	54.2
10	1.84	0.96	0.29	0.84	2.18	54.7
11	1.86	0.96	0.30	0.85	2.19	54.9
12	1.86	0.96	0.30	0.85	2.18	54.8
13	1.83	0.96	0.29	0.84	2.18	54.7
14	1.85	0.96	0.30	0.85	2.17	54.4
15	1.82	0.96	0.29	0.84	2.17	54.3
				AVG.	2.17	54.5
				S.D.	0.02	0.39

APPENDIX D

Sintered density of composition A, B and C at various sintering temperature

Sintering temperature: 1275°C

Number	Dry weight (g)	Weight in water (g)	Wet weight (g)	Density (g/cm^3)	Relative density (%)	AVG.	S.D.
A10	1.80	1.33	1.82	3.65	91.8	92.0	0.6
A11	1.81	1.35	1.84	3.64	91.5		
A12	1.85	1.37	1.87	3.69	92.6		
B10	1.82	1.36	1.87	3.51	88.0	88.0	0.1
B11	1.82	1.36	1.87	3.51	88.1		
B12	1.81	1.35	1.87	3.50	87.9		
C10	1.83	1.36	1.90	3.39	85.0	85.1	0.1
C11	1.84	1.38	1.92	3.40	85.2		
C12	1.84	1.37	1.91	3.39	85.0		

Sintering temperature: 1300°C

Number	Dry weight (g)	Weight in water (g)	Wet weight (g)	Density (g/cm^3)	Relative density (%)	AVG.	S.D.
A4	1.82	1.34	1.83	3.77	94.8	95.0	0.3
A5	1.83	1.35	1.84	3.78	95.0		
A6	1.80	1.33	1.80	3.79	95.3		
B4	1.82	1.35	1.85	3.64	91.3	91.2	0.4
B5	1.82	1.36	1.85	3.65	91.6		
B6	1.84	1.36	1.87	3.62	90.8		
C4	1.80	1.34	1.85	3.52	88.3	88.6	0.3
C5	1.80	1.35	1.85	3.54	88.7		
C6	1.81	1.35	1.86	3.55	88.9		

Sintering temperature: 1350°C

Number	Dry weight (g)	Weight in water (g)	Wet weight (g)	Density (g/cm^3)	Relative density (%)	AVG.	S.D.
A13	1.84	1.38	1.84	3.93	98.7	98.7	0.1
A14	1.82	1.36	1.82	3.92	98.6		
A15	1.83	1.37	1.83	3.93	98.8		
B13	1.83	1.36	1.84	3.80	95.5	95.6	0.1
B14	1.83	1.35	1.83	3.81	95.7		
B15	1.82	1.35	1.83	3.81	95.7		
C13	1.81	1.34	1.82	3.78	94.8	94.7	0.2
C14	1.83	1.36	1.84	3.77	94.5		
C15	1.80	1.33	1.81	3.78	94.7		

Sintering temperature: 1400°C

Number	Dry weight (g)	Weight in water (g)	Wet weight (g)	Density (g/cm^3)	Relative density (%)	AVG.	S.D.
A1	1.85	1.39	1.85	3.95	99.4	99.2	0.2
A2	1.87	1.40	1.88	3.94	99.1		
A3	1.84	1.38	1.84	3.94	99.0		
B1	1.85	1.38	1.85	3.94	98.8	98.5	0.4
B2	1.86	1.39	1.87	3.91	98.0		
B3	1.87	1.39	1.87	3.93	98.6		
C1	1.82	1.36	1.82	3.90	97.8	97.8	0.1
C2	1.82	1.36	1.83	3.90	97.8		
C3	1.84	1.37	1.84	3.90	97.9		

Sintering temperature: 1450°C

Number	Dry weight (g)	Weight in water (g)	Wet weight (g)	Density (g/cm^3)	Relative density (%)	AVG.	S.D.
A4	1.83	1.37	1.83	3.96	99.4	99.1	0.2
A5	1.84	1.38	1.85	3.94	98.9		
A6	1.84	1.38	1.84	3.94	99.1		
B4	1.84	1.38	1.84	3.91	98.2	98.9	0.7
B5	1.81	1.35	1.81	3.94	98.8		
B6	1.86	1.40	1.86	3.97	99.6		
C4	1.85	1.38	1.85	3.97	99.6	99.2	0.5
C5	1.76	1.32	1.76	3.96	99.3		
C6	1.91	1.43	1.92	3.93	98.6		

Sintering temperature: 1500°C

Number	Dry weight (g)	Weight in water (g)	Wet weight (g)	Density (g/cm^3)	Relative density (%)	AVG.	S.D.
A7	1.84	1.38	1.85	3.94	98.9	98.7	0.2
A8	1.85	1.39	1.85	3.93	98.9		
A9	1.87	1.40	1.87	3.92	98.5		
B7	1.86	1.39	1.86	3.96	99.3	99.3	0.2
B8	1.88	1.41	1.88	3.96	99.4		
B9	1.84	1.38	1.84	3.95	99.1		
C7	1.84	1.39	1.85	3.99	100.0	99.3	0.6
C8	1.85	1.39	1.85	3.96	99.2		
C9	1.82	1.37	1.83	3.94	98.8		

APPENDIX E

Sintered density of specimen at various sintering temperature and soaking time

Sintering condition	Dry weight (g)	Weight in water (g)	Wet weight (g)	Density (g/cm^3)	Relative density (%)	AVG.	S.D.
1350×2.0 hr							
1	2.72	2.03	2.72	3.92	98.6	98.5	0.2
2	2.71	2.03	2.72	3.93	98.6		
3	2.71	2.03	2.72	3.91	98.2		
1350×1.0 hr							
1	2.72	2.03	2.72	3.89	97.8	97.7	0.2
2	2.73	2.03	2.73	3.89	97.8		
3	2.75	2.05	2.76	3.88	97.5		
1350×0.5 hr							
1	2.73	2.02	2.74	3.82	96.0	96.0	0.4
2	2.75	2.04	2.75	3.84	96.4		
3	2.71	2.01	2.72	3.80	95.6		
1300×2.0 hr							
1	2.73	2.02	2.74	3.82	95.8	95.9	0.1
2	2.69	1.99	2.69	3.83	96.0		
3	2.79	2.07	2.80	3.82	95.8		
1300×1.0 hr							
1	2.71	2.00	2.73	3.70	92.9	93.0	0.1
2	2.68	1.99	2.71	3.70	93.0		
3	2.70	2.00	2.72	3.70	93.0		
1300×0.5 hr							
1	2.73	2.04	2.81	3.55	89.1	89.1	0.1
32	2.72	2.03	2.80	3.54	89.0		
3	2.72	2.03	2.79	3.55	89.3		

APPENDIX F

Experimental Result of Microwave Sintering in TAKASAGO

Sample No.	Sintering Temperature (°C)	Soaking Time (min.)	Heating Rate (°C/min.)	Relative Density (%)
1,2	1250	120	10	94.3, 94.6
3,4	1300	120	10	97.5, 97.7
5,6	1350	120	10	98.9, 98.2
7,8	1400	120	10	99.9, 99.8
9,10	1275	120	10	96.7, 96.4
11,12	1325	120	10	98.6, 98.598.4
13,14	1300	60	10	96.3, 96.2
15,16	1300	30	10	95.6, 94.4
17,18	1300	120	30	97.7, 97.5
19,20	1300	120	50	97.2, 97.7
21,22	1300	30	50	95.7, 95.2

APPENDIX G

Density of specimen prepared by Microwave and Conventional method and followed by sinter-HIP at 1300°C×1 hr×10°C /min

Microwave sintering	Dry weight (g)	Weight in water (g)	Wet weight (g)	Density (g/cm^3)	Relative density (%)
1250°C×120 min×10°C /min (MW2)	2.72	2.04	2.72	3.97	99.7
1275°C×120 min×10°C /min (MW9)	2.71	2.04	2.72	3.96	99.5
1300°C×120 min×10°C /min (MW4)	2.71	2.03	2.71	3.96	99.4
1300°C×60 min×10°C /min (MW14)	2.76	2.07	2.77	3.94	99.1
1300°C×30 min×10°C /min (MW15)	2.74	2.05	2.74	3.95	99.3
1300°C×120 min×50°C /min (MW19)	2.71	2.03	2.71	3.95	99.2
1300°C×30 min×50°C /min (MW22)	2.71	2.03	2.72	3.97	99.8
1325°C×120 min×10°C /min (MW11)	2.71	2.03	2.71	3.95	99.2
1350°C×120 min×10°C /min (MW5)	2.72	2.04	2.72	3.95	99.3
1400°C×120 min×10°C /min (MW7)	2.71	2.03	2.71	3.98	99.9

Conventional sintering	Dry weight (g)	Weight in water (g)	Wet weight (g)	Density (g/cm^3)	Relative density (%)
1275°C×120 min×10°C /min (S5)	2.72	2.04	2.72	3.98	100.0
1300°C×120 min×10°C /min (S2)	2.65	1.99	2.65	3.98	100.0
1300°C×120 min×10°C /min (A5)	1.83	1.38	1.84	3.93	98.9
1350°C×120 min×10°C /min (S7)	2.69	2.02	2.69	3.97	99.7
1350°C×120 min×10°C /min (A13)	1.84	1.38	1.85	3.95	99.2
1350°C×120 min×10°C /min (B13)	1.83	1.37	1.83	3.96	99.5
1350°C×120 min×10°C /min (C13)	1.81	1.35	1.82	3.92	98.3
1400°C×120 min×10°C /min (A2)	1.87	1.40	1.87	3.96	99.5
1400°C×120 min×10°C /min (B2)	1.86	1.39	1.86	3.94	99.0
1400°C×120 min×10°C /min (C2)	1.83	1.36	1.83	3.94	98.7

Density of specimens before and after HIP at 1300°C×1 hr×10°C /min

Microwave sintering	Relative density (%)	
	Before HIP	After HIP
1250°C×120 min×10°C /min (MW2)	94.6	99.7
1275°C×120 min×10°C /min (MW9)	96.7	99.5
1300°C×120 min×10°C /min (MW4)	97.7	99.4
1300°C×60 min×10°C /min (MW14)	96.2	99.1
1300°C×30 min×10°C /min (MW15)	95.6	99.3
1300°C×120 min×50°C /min (MW19)	97.2	99.2
1300°C×30 min×50°C /min (MW22)	95.2	99.8
1325°C×120 min×10°C /min (MW11)	98.6	99.2
1350°C×120 min×10°C /min (MW5)	98.9	99.3
1400°C×120 min×10°C /min (MW7)	99.9	99.9

Conventional sintering	Relative density (%)	
	Before HIP	After HIP
1275°C×120 min×10°C /min (S5)	96.7	100.0
1300°C×120 min×10°C /min (S2)	96.0	100.0
1300°C×120 min×10°C /min (A5)	94.0	98.9
1350°C×120 min×10°C /min (S7)	99.1	99.7
1350°C×120 min×10°C /min (A13)	98.7	99.2
1350°C×120 min×10°C /min (B13)	95.5	99.5
1350°C×120 min×10°C /min (C13)	94.8	98.3
1400°C×120 min×10°C /min (A2)	99.1	99.5
1400°C×120 min×10°C /min (B2)	98.0	99.0
1400°C×120 min×10°C /min (C2)	97.8	98.7

APPENDIX H

Effect of HIP condition on sinter density

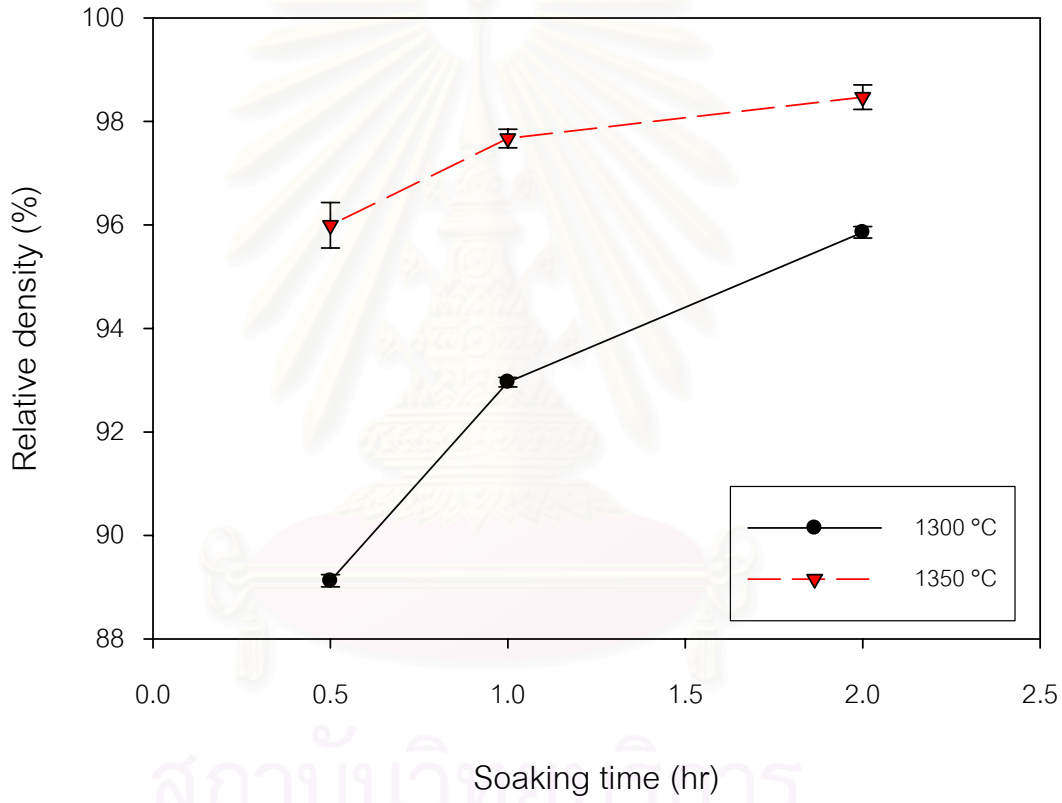

Sintered density of conventional specimens

HIP: 1250°C×1 hr×10°C /min

Sintering condition	Dry weight (g)	Weight in water (g)	Wet weight (g)	Density (g/cm^3)	Relative density (%)
1300°C×60 min×10°C /min	2.70	2.01	2.71	3.87	97.2
1300°C×120 min×10°C /min	2.73	2.04	2.73	3.94	99.0
1350°C×30 min×10°C /min	2.73	2.05	2.74	3.96	99.4
1350°C×60 min×10°C /min	2.72	2.04	2.72	3.97	99.7
1350°C×120 min×10°C /min	2.72	2.04	2.72	3.96	99.6

HIP: 1300°C×0.5 hr×10°C /min

Sintering condition	Dry weight (g)	Weight in water (g)	Wet weight (g)	Density (g/cm^3)	Relative density (%)
1300°C×60 min×10°C /min	2.68	1.99	2.69	3.86	97.0
1300°C×120 min×10°C /min	2.79	2.09	2.79	3.96	99.5
1350°C×30 min×10°C /min	2.71	2.03	2.71	3.97	99.8
1350°C×60 min×10°C /min	2.73	2.05	2.73	3.97	99.8
1350°C×120 min×10°C /min	2.71	2.03	2.71	3.97	99.8

HIP: 1300°C×1 hr×10°C /min

Sintering condition	Dry weight (g)	Weight in water (g)	Wet weight (g)	Density (g/cm^3)	Relative density (%)
1300°C×60 min×10°C /min	2.47	1.83	2.47	3.86	96.9
1300°C×120 min×10°C /min	2.46	1.84	2.46	3.95	99.3
1350°C×30 min×10°C /min	2.59	1.94	2.60	3.96	99.5
1350°C×60 min×10°C /min	2.60	1.95	2.61	3.96	99.6
1350°C×120 min×10°C /min	2.57	1.93	2.58	3.98	100.0

APPENDIX G

Transparency of conventional and microwave specimens

Wavelength	% Transmittance					
	CV-1	CV-2	CV-3	CV-4	CV-5	CV-6
200	0.02	0.02	0.02	0.03	0.03	0.03
250	0.19	0.14	0.19	0.27	0.24	0.23
300	0.82	0.50	0.79	0.99	0.91	0.70
350	2.05	1.13	2.13	2.24	2.42	1.44
400	4.20	1.99	4.23	4.29	4.75	2.30
450	6.94	3.34	7.18	6.85	7.96	3.49
500	10.42	5.21	11.01	10.05	12.05	5.03
550	18.38	10.01	19.88	17.31	21.37	8.96
600	18.38	10.01	19.88	17.31	21.37	8.96
650	22.50	12.78	24.50	21.08	26.14	11.30
700	26.54	15.68	29.02	24.81	30.78	13.84
750	30.43	18.62	33.33	28.42	35.16	16.53
800	34.12	21.57	37.37	31.86	39.24	19.33
850	37.59	24.48	41.14	35.14	43.02	22.19
900	40.83	27.31	44.63	38.22	46.50	25.05
950	43.82	30.07	47.81	41.08	49.66	27.88
1000	46.59	32.72	50.73	43.79	52.55	30.66
1050	49.17	35.26	53.43	46.28	55.21	33.40
1100	51.46	37.64	55.78	48.57	57.53	35.98

Wavelength	% Transmittance			
	MW-1	MW-2	MW-3	MW-4
200	0.01	0.01	0.01	0.01
250	0.07	0.02	0.06	0.06
300	0.23	0.11	0.24	0.24
350	0.43	0.34	0.49	0.37
400	0.34	0.16	0.48	0.38
450	0.42	0.18	0.77	0.52
500	0.53	0.19	1.37	0.81
550	0.70	0.20	2.37	1.33
600	0.93	0.21	3.85	2.15
650	1.25	0.23	5.85	3.34
700	1.68	0.26	8.32	4.91
750	2.22	0.29	11.17	6.83
800	2.91	0.32	14.32	9.08
850	3.76	0.37	17.68	11.61
900	4.75	0.42	21.16	14.36
950	5.90	0.50	24.67	17.26
1000	7.22	0.58	28.21	20.30
1050	8.67	0.70	31.58	23.31
1100	10.26	0.87	34.85	26.31

BIOGRAPHY

Miss Jutinun Kraikrer was born in Trang, Thailand on January 9th, 1980. In 2002, she finished her Bachelor Degree in Physics from the Department of Physics, Faculty of Science, Thaksin University. After that, she was a teaching and research assistant at school of physics, Institute of Science, Suranaree University of Technology for 2 years. In 2004, she left to study for Master's Degree in the field of Ceramic Technology at Chulalongkorn University and graduated in 2006.